Computer-Aided Civil and Infrastructure Engineering **24** (2009) 470–491

Identification of Time-Variant Modal Parameters Using Time-Varying Autoregressive with Exogenous Input and Low-Order Polynomial Function

C. S. Huang*, S. L. Hung & W. C. Su
Department of Civil Engineering, National Chiao Tung University, Hsinchu, Taiwan

&

C. L. Wu
National Center for Research on Earthquake Engineering, Taipei, Taiwan

Abstract: *This work presents an approach that accurately identifies instantaneous modal parameters of a structure using time-varying autoregressive with exogenous input (TVARX) model. By developing the equivalent relations between the equation of motion of a time-varying structural system and the TVARX model, this work proves that instantaneous modal parameters of a time-varying system can be directly estimated from the TVARX model coefficients established from displacement responses. A moving least-squares technique incorporating polynomial basis functions is adopted to approximate the coefficient functions of the TVARX model. The coefficient functions of the TVARX model are represented by polynomials having time-dependent coefficients, instead of constant coefficients as in traditional basis function expansion approaches, so that only low orders of polynomial basis functions are needed. Numerical studies are carried out to investigate the effects of parameters in the proposed approach on accurately determining instantaneous modal parameters. Numerical analyses also demonstrate that the proposed approach is superior to some published techniques (i.e., recursive technique with a forgetting factor, traditional basis function expansion approach, and weighted basis function expansion approach) in accurately estimating instantaneous modal parameters of a structure. Finally, the proposed approach is applied to process measured data for a frame specimen subjected to a series of base excitations in shaking table tests. The specimen was damaged during testing. The identified instantaneous modal parameters are consistent with observed physical phenomena.*

*To whom correspondence should be addressed. E-mail: *cshuang@mail.nctu.edu.tw*.

DOI: 10.1111/j.1467-8667.2009.00605.x

1 INTRODUCTION

Time-varying systems have many applications in various fields. In mechanical and civil engineering, a system with active control devices (Saleh and Adeli, 1994, 1997, 1998; Adeli and Saleh, 1997, 1998; Adeli and Kim, 2004; Kim and Adeli, 2004, 2005a,b,c,d; Jiang and Adeli, 2008a,b) modifying stiffness or damping is a time-varying system. A structure under damage normally exhibits nonlinear dynamic behaviors and time-dependent stiffness and damping (e.g., Adeli and Jiang, 2006; Jiang et al., 2007). Variations in system stiffness and damping over time result in time-varying modal parameters of the system. Consequently, determining instantaneous modal parameters of a time-varying system is generally very useful when assessing structural damage in real applications.

The time-varying autoregressive with exogenous input (TVARX) model is often utilized to establish an input–output relationship of a time-varying linear system from its dynamic responses and input forces (e.g.,

Loh et al., 2000; Niedźwiecki, 2000). The recursive least-squares approach is one of the most popular techniques to estimate time-dependent coefficients of the TVARX model. The recursive least-squares approach, which is an online approach, was well described by Ljung (1987). Although the recursive least-squares approach has high computational efficiency when estimating time-varying parameters, the approach shows slow tracking capability for time-varying coefficients and is highly sensitive to initial conditions. To improve these shortcomings, variable forgetting factors (Fortescue et al., 1981; Toplis and Pasupathy, 1988; Leung and So, 2005), covariance matrix resetting (Jiang and Cook, 1992; Park and Jun, 1992), the sliding window technique (Choi and Bien, 1989; Belge and Miller, 2000), and Kalman filter (Loh et al., 2000) have been incorporated into the recursive least-squares approach.

Another common approach for establishing the TVARX model is the basis function expansion approach, which shows excellent capability on tracking coefficients changing with time. Various basis functions, such as the Fourier series (Marmarelis, 1987), Legendre polynomial (Niedźwiecki, 1988), Walsh function (Zou et al., 2003), and wavelets (Tsatsanis and Giannakis, 1993; Wei and Billings, 2002; Adeli and Samant, 2000; Karim and Adeli, 2002; Ghosh-Dastidar and Adeli, 2003), were used to describe TVARX model coefficients. Selecting the proper basis functions is a key to the success of this approach. Numerical experiences by Zou et al. (2003) indicated that the Legendre polynomial performed well for the coefficients that change smoothly over time, whereas the Walsh functions were good for piecewise stationary time-varying coefficients. The basis function expansion approach often needs a great number of basis functions and always has trouble determining how many basis functions should be used. Numerical difficulties are often encountered when a large number of basis functions are utilized, especially for polynomial basis functions. Niedźwiecki (2000) proposed a weighted basis function approach to overcome these problems, but his approach has an inherent drawback of computational inefficiency in establishing the TVARX model.

Accurately establishing the TVARX model from measured dynamic responses of a structure is inadequate for assessing structural damage even though most published work on the TVARX model is concerned with how to establish the model accurately. Furthermore, the TVARX model coefficients do not have physical meanings. A popular approach to assess structural damage is based on the changes of modal parameters of the structure (Moaveni et al., 2008; Carden and Brownjohn, 2008; He et al., 2008; Li and Wu, 2008; Ni et al., 2008) even though a drop in natural frequency itself may not really result from structural damage (Clinton et al., 2006). Consequently, this work presents a novel procedure for accurately determining instantaneous modal parameters of a time-varying system.

First, this work describes a novel and efficient approach for constructing a suitable TVARX model from the dynamic responses of a structure. The coefficient functions in the TVARX model are constructed through the moving least-squares technique adapted from the mesh-free finite element method for constructing shape functions (Liu, 2003). The proposed approach needs only low-order polynomials to accurately approximate TVARX model coefficients and considerably improves the computational inefficiency of a weighted basis function approach.

Second, this work verifies the equivalence between the equation of motion for a structure and the TVARX model when displacement, velocity, or acceleration responses are utilized. Then, this work demonstrates, for the first time in publication, that the instantaneous modal parameters of a time-varying system can be estimated from TVARX model coefficients established using displacement responses but not using velocity or acceleration responses by a traditional technique typically used for the AR or ARX model for estimating modal parameters.

Numerical simulations are performed to validate the effectiveness of the proposed procedure in estimating instantaneous modal parameters accurately. Numerical studies investigate the effects of parameters in the proposed procedure on accurate determination of instantaneous modal parameters. Numerical studies also indicate that the proposed approach is superior to some published techniques (i.e., recursive technique with a forgetting factor, traditional basis function expansion approach, and weighted basis function expansion approach) in providing accurate estimation of instantaneous modal parameters for a structure. Finally, the proposed procedure is applied to process measured data for a frame specimen, subjected to a series of base excitations in shaking table tests. The specimen showed strong nonlinear dynamic behaviors because damage occurred during testing.

2 METHODOLOGY

The time-varying structural system encountered in civil and mechanical engineering can be described by the following equation of motion when a single-degree-of-freedom system is considered:

$$m(t)\ddot{x} + c(t)\dot{x} + k(t)x = f(t) \tag{1}$$

where m, c, and k are system mass, damping coefficient, and stiffness, respectively; $\ddot{x}$, $\dot{x}$, and x are

acceleration, velocity, and displacement, respectively. The time-dependent material properties of the system m, c, and k are likely due to control devices or imposed damage.

The instantaneous modal parameters of a time-varying system given by Equation (1) are defined,

$$\omega_n(t) = 2\pi f_n(t) = \sqrt{\frac{k(t)}{m(t)}} \quad \text{and} \quad \xi(t) = \frac{c(t)}{2m(t)\omega_n(t)} \tag{2}$$

where $\omega_n(t)$ and $\xi(t)$ are instantaneous natural frequency and damping ratio, respectively, and are time dependent. These definitions are similar to those of modal parameters for a linear time-invariant (LTI) system. Consequently, the system given by Equation (1) can also be characterized by its instantaneous modal parameters.

When the output responses and input of a time-varying system are measured, the TVARX model is frequently applied to establish the relationship between measured input and output. The mathematical expression of the TVARX model with the order (I, J), TVARX(I, J) for single-input/output systems (or systems with a single degree of freedom) is

$$y(t) = \sum_{i=1}^{I} \phi_i(t) y(t-i) + \sum_{j=0}^{J} \theta_j(t) f(t-j) + a_n(t) \tag{3}$$

where $y(t-i)$ and $f(t-i)$ are the measured response, which can be acceleration, velocity or displacement, and input at time $t - i\Delta t$, respectively; $1/\Delta t$ is the sampling rate of the measurement; $\phi_i(t)$ and $\theta_j(t)$ are coefficient functions to be determined in the model; $a_n(t)$ is the residual error accommodating the effects of measurement noise, modeling errors, and unmeasured disturbances. The relationship between Equations (1) and (3) is examined in the following section.

A moving least-squares approach (Lancaster and Šalkauskas, 1990) is employed to construct the coefficient functions. The TVARX model coefficient functions are expanded onto a set of basis functions. Approximation theory of a function states that a function can always be expanded by a complete set of basis functions (Watson, 1980). Hence, polynomial basis functions are used here; let

$$\phi_i(t) = \sum_{n=0}^{N_i} \bar{a}_{in} t^n = \boldsymbol{p}_i^T \boldsymbol{a}_i \quad \text{and} \quad \theta_j(t) = \sum_{n=0}^{\bar{N}_j} \bar{b}_{jn} t^n = \bar{\boldsymbol{p}}_j^T \boldsymbol{b}_j \tag{4}$$

where $\boldsymbol{p}_i^T = (1, t, t^2, \ldots, t^{N_i})$, $\bar{\boldsymbol{p}}_j^T = (1, t, t^2, \ldots, t^{\bar{N}_j})$, $\boldsymbol{a}_i^T = (\bar{a}_{i0}, \bar{a}_{i1}, \bar{a}_{i2}, \ldots, \bar{a}_{iN_i})$, $\boldsymbol{b}_j^T = (\bar{b}_{j0}, \bar{b}_{j1}, \bar{b}_{j2}, \ldots, \bar{b}_{j\bar{N}_j})$; $\bar{a}_{in}$ and $\bar{b}_{jn}$ are the coefficients to be determined.

A weighted least-squares technique is applied to determine coefficients $\bar{a}_{in}$ and $\bar{b}_{jn}$ in Equation (4). Let $\bar{\phi}_{ik}$ and $\bar{\theta}_{jk}$ denote the true values of $\phi_i(t_k)$ and $\theta_j(t_k)$, respectively. Vector $\boldsymbol{a}_i$ is determined by minimizing the error function defined by

$$E(t) = \sum_{l=1}^{\bar{l}_i} W(t, t_l) \left(\boldsymbol{p}_i^T(t_l) \boldsymbol{a}_i - \bar{\phi}_{il} \right)^2 \tag{5}$$

where $W(t, t_l)$ is a weight function that must be positive, and $\bar{l}_i$ is the number of nodal points for $\phi_i(t)$. The nodal points uniformly distribute along the time domain under consideration.

Minimizing E yields

$$\frac{\partial E}{\partial \boldsymbol{a}_i} = \boldsymbol{0} \tag{6}$$

Careful arrangement of Equation (6) yields

$$\boldsymbol{A}_i(t) \boldsymbol{a}_i = \boldsymbol{Q}_i(t) \bar{\boldsymbol{\varphi}}_i \tag{7}$$

where

$$\boldsymbol{A}_i(t) = \sum_{l=1}^{\bar{l}_i} W(t, t_l) \boldsymbol{p}_i(t_l) \boldsymbol{p}_i^T(t_l), \quad \boldsymbol{Q}_i(t) = [\boldsymbol{q}_{i1}, \boldsymbol{q}_{i2}, \ldots, \boldsymbol{q}_{i\bar{l}_i}].$$

$$\boldsymbol{q}_{il} = W(t, t_l) \boldsymbol{p}_i(t_l) \quad \text{and} \quad \bar{\boldsymbol{\varphi}}_i = (\bar{\phi}_{i1}, \bar{\phi}_{i2}, \ldots, \bar{\phi}_{i\bar{l}_i})^T \tag{8}$$

The solution for $\boldsymbol{a}_i$ in Equation (7) is

$$\boldsymbol{a}_i = \boldsymbol{A}_i^{-1}(t) \boldsymbol{Q}_i(t) \bar{\boldsymbol{\varphi}}_i \tag{9}$$

Equation (9) indicates that $\boldsymbol{a}_i$ is dependent on time. Notably, the number of nodal points should be much larger than the number of basis functions in $\boldsymbol{p}_i$ to ensure the existence of $\boldsymbol{A}_i^{-1}$. Substituting Equation (9) into Equation (4) results in

$$\phi_i(t) = \tilde{\boldsymbol{\varphi}}_i(t) \bar{\boldsymbol{\varphi}}_i \tag{10}$$

where $\tilde{\boldsymbol{\varphi}}_i(t)$ is a vector of shape functions for $\phi_i(t)$ in terms of finite element terminology, and

$$\tilde{\boldsymbol{\varphi}}_i(t) = \boldsymbol{p}_i^T(t) \boldsymbol{A}_i^{-1}(t) \boldsymbol{Q}_i(t) \tag{11}$$

Similarly, $\theta_j(t)$ can be expressed as

$$\theta_j(t) = \tilde{\boldsymbol{\theta}}_j(t) \bar{\boldsymbol{\vartheta}}_j \tag{12}$$

where

$$\bar{\boldsymbol{\vartheta}}_j = (\bar{\theta}_{j1}, \bar{\theta}_{j2}, \ldots, \bar{\theta}_{j\hat{l}_j})^T, \ \tilde{\boldsymbol{\theta}}_j(t) = \bar{\boldsymbol{p}}_j^T(t) \bar{\boldsymbol{A}}_j^{-1}(t) \bar{\boldsymbol{Q}}_j(t).$$

$$\bar{\boldsymbol{A}}_j(t) = \sum_{l=1}^{\hat{l}_j} W(t, t_l) \bar{\boldsymbol{p}}_j(t_l) \bar{\boldsymbol{p}}_j^T(t_l), \ \bar{\boldsymbol{Q}}_j(t) = [\bar{\boldsymbol{q}}_{j1}, \bar{\boldsymbol{q}}_{j2}, \ldots, \bar{\boldsymbol{q}}_{j\hat{l}_j}]$$

$$\bar{\boldsymbol{q}}_{jl} = W(t, t_l) \bar{\boldsymbol{p}}_j(t_l) \tag{13}$$

and $\hat{l}_j$ is the number of nodal points for $\theta_j(t)$. If the same nodal points and the same polynomial bases are used

for each coefficient function in the TVARX model, each coefficient function has the same shape functions, and the formulation becomes simple. In Equations (10) and (12), $\bar{\varphi}_i$ and $\bar{\vartheta}_j$ are unknown. Notably, the number of nodal points should be much larger than the number of basis functions in $\boldsymbol{p}_i$.

A least-squares approach is applied to determine $\bar{\boldsymbol{\varphi}}_i$ and $\bar{\boldsymbol{\vartheta}}_j$ by minimizing

$$\bar{E} = \sum_{\bar{n}=1}^{N} (a_n(t_{\bar{n}}))^2 \tag{14}$$

where N is the number of data points to be used in establishing the TVARX model. Recall that $a_n(t)$ is the noise variable in the TVARX model. From Equations (3), (11), and (12), one can establish

$$a_n(t) = y(t) - \left(\sum_{i=1}^{I} \boldsymbol{\Gamma}_{t,i} \bar{\boldsymbol{\varphi}}_i + \sum_{j=0}^{J} \boldsymbol{\Pi}_{t,j} \bar{\boldsymbol{\vartheta}}_j \right) \tag{15}$$

where

$$\boldsymbol{\Gamma}_{t,i} = y(t-i)\,\tilde{\boldsymbol{\varphi}}_i(t) \quad \text{and} \quad \boldsymbol{\Pi}_{t,j} = f(t-j)\,\tilde{\boldsymbol{\theta}}_j(t) \tag{16}$$

Substituting Equations (15) and (16) into Equation (14) and minimizing $\bar{E}$ with respect to $\bar{\varphi}_i$ and $\bar{\vartheta}_j$ yield

$$\boldsymbol{V}^T \tilde{\boldsymbol{Y}} = \boldsymbol{V}^T \boldsymbol{V} \tilde{\boldsymbol{C}} \tag{17}$$

where

$$\boldsymbol{V} = \begin{bmatrix} \boldsymbol{\Gamma}_{t_1,1} & \boldsymbol{\Gamma}_{t_1,2} & \cdots & \boldsymbol{\Gamma}_{t_1,I} & \boldsymbol{\Pi}_{t_1,0} & \boldsymbol{\Pi}_{t_1,1} & \cdots & \boldsymbol{\Pi}_{t_1,J} \\ \boldsymbol{\Gamma}_{t_2,1} & \boldsymbol{\Gamma}_{t_2,2} & \cdots & \boldsymbol{\Gamma}_{t_2,I} & \boldsymbol{\Pi}_{t_2,0} & \boldsymbol{\Pi}_{t_2,1} & \cdots & \boldsymbol{\Pi}_{t_2,J} \\ \vdots & \vdots & \ddots & \vdots & \vdots & \vdots & \ddots & \vdots \\ \boldsymbol{\Gamma}_{t_N,1} & \boldsymbol{\Gamma}_{t_N,2} & \cdots & \boldsymbol{\Gamma}_{t_N,I} & \boldsymbol{\Pi}_{t_N,0} & \boldsymbol{\Pi}_{t_N,1} & \cdots & \boldsymbol{\Pi}_{t_N,J} \end{bmatrix} \tag{18a}$$

$$\tilde{\boldsymbol{Y}} = \begin{bmatrix} y(t_1) & y(t_2) & \cdots & y(t_N) \end{bmatrix}^T \tag{18b}$$

$$\tilde{\boldsymbol{C}} = \begin{bmatrix} \bar{\boldsymbol{\varphi}}_1^T & \bar{\boldsymbol{\varphi}}_2^T & \cdots & \bar{\boldsymbol{\varphi}}_I^T & \bar{\boldsymbol{\vartheta}}_0^T & \bar{\boldsymbol{\vartheta}}_1^T & \cdots & \bar{\boldsymbol{\vartheta}}_J^T \end{bmatrix}^T \tag{18c}$$

Unknowns $\bar{\varphi}_i$ and $\bar{\vartheta}_j$ are determined from Equation (17) by

$$\tilde{\boldsymbol{C}} = (\boldsymbol{V}^T \boldsymbol{V})^{-1} \boldsymbol{V}^T \tilde{\boldsymbol{Y}} \tag{19}$$

Then, coefficient functions $\phi_i(t)$ in the TVARX model, Equation (3), are derived by substituting Equation (19) into Equation (10).

Many weight functions can be used in the above formulation (Lancaster and Šalkauskas, 1990; Liu, 2003). In this work, the exponential weight function is applied:

$$W(t_m, t_p) = \begin{cases} e^{-((t_m - t_p)/0.3d)^2} & |t_m - t_p|/d \le 1 \\ 0 & |t_m - t_p|/d > 1 \end{cases} \tag{20}$$

where d defines the dimension of the domain where $W \neq 0$ and is called the support of the weight function. This weight function is usually used in curve fitting (Lancaster and Šalkauskas, 1990) or constructing shape functions in the mesh-free method (Liu, 2003).

It is desirable to obtain instantaneous modal parameters of the time-varying system after the TVARX model has been established from measured output and input. Instantaneous modal parameters can be evaluated by following the same procedure used to estimate modal parameters for an LTI system from the ARX model (Wang and Fang, 1986; Huang, 2001) because the TVARX model is exactly the same as the ARX model at any instantaneous moment. Consequently, the instantaneous modal parameters are associated with the poles of

$$\left| \lambda^I - \lambda^{I-1}\phi_1 - \lambda^{I-2}\phi_2 - \cdots - \lambda\phi_{I-1} \right| = 0 \tag{21}$$

Because ϕ_j ($j = 1, 2, \ldots, I$) is time dependent, the poles $\boldsymbol{\lambda}$ are also functions of time. The values of $\boldsymbol{\lambda}$ are usually complex and appear in a conjugate pair. Let λ_k be a root of Equation (21) and $\lambda_k = c_k + id_k$. Then, the corresponding instantaneous natural frequency and damping ratio are determined by

$$\omega_k = \sqrt{\alpha_k^2 + \beta_k^2} \quad \text{and} \quad \xi_k = \frac{\alpha_k}{\omega_k} \tag{22}$$

where

$$\beta_k = \frac{1}{\Delta t} \tan^{-1} \frac{d_k}{c_k} \quad \text{and} \quad \alpha_k = \frac{1}{2\Delta t} \ln(c_k^2 + d_k^2) \tag{23}$$

Notably, the system given by Equation (1) with a single degree of freedom should have only one instantaneous natural frequency function. Consequently, I in Equation (21), or Equation (3), should theoretically equal two, and only two roots for Equation (21) exist. However, I in Equation (21) is typically larger than two when the responses or input containing noise are employed to construct the TVARX model.

3 TVARX MODEL AND STRUCTURAL DYNAMIC RESPONSES

This section establishes the theoretical relationship between Equations (1) and (3) and further assesses the validity of the procedure in determining the instantaneous modal parameters shown in the previous section.

According to the central difference approach, Equation (1) can be discretized as

$$\left[\frac{m(t)}{(\Delta t)^2} + \frac{c(t)}{2\Delta t} \right] x(t + \Delta t) = f(t) - \left[k(t) - \frac{2m(t)}{(\Delta t)^2} \right] x(t) - \left[\frac{m(t)}{(\Delta t)^2} - \frac{c(t)}{2\Delta t} \right] x(t - \Delta t) \tag{24}$$

The equation is further simplified as

$$x(t) = \hat{\phi}_1(t)x(t-\Delta t) + \hat{\phi}_2 x(t-2\Delta t) + \hat{\theta}_1(t) f(t-\Delta t) \tag{25}$$

where

$$\hat{\phi}_1(t) = -\frac{k(t-\Delta t) - 2m(t-\Delta t)/(\Delta t)^2}{\gamma(t-\Delta t)},$$

$$\hat{\phi}_2(t) = -\frac{m(t-\Delta t)/(\Delta t)^2 - c(t-\Delta t)/(2\Delta t)}{\gamma(t-\Delta t)},$$

$$\hat{\theta}_1(t) = \frac{1}{\gamma(t-\Delta t)} \quad \text{and}$$

$$\gamma(t-\Delta t) = \frac{m(t-\Delta t)}{(\Delta t)^2} + \frac{c(t-\Delta t)}{(2\Delta t)} \tag{26}$$

If velocity responses are utilized to establish the discrete equation of Equation (1), differentiating Equation (1) with respect to t once yields

$$m(t)\ddot{v}(t) + [\dot{m}(t) + c(t)]\dot{v}(t) + [\dot{c}(t) + k(t)]v(t) + \dot{k}(t)x(t) = \dot{f}(t) \tag{27}$$

where $v(t)$ denotes velocity responses. From Equation (1),

$$x(t) = \frac{1}{k(t)}[f(t) - m(t)\dot{v}(t) - c(t)v(t)] \tag{28}$$

Substituting Equation (28) into Equation (27) and using the central difference approach lead to

$$v(t) = \breve{\phi}_1(t)v(t-\Delta t) + \breve{\phi}_2(t)v(t-2\Delta t) + \breve{\theta}_0(t)f(t) + \breve{\theta}_1(t)f(t-\Delta t) + \breve{\theta}_2(t)f(t-2\Delta t) \tag{29}$$

where

$$\breve{\phi}_1(t) = -\frac{\breve{k}(t-\Delta t) - 2m(t-\Delta t)/(\Delta t)^2}{\breve{\gamma}(t-\Delta t)},$$

$$\breve{\phi}_2(t) = -\frac{m(t-\Delta t)/(\Delta t)^2 - \breve{c}(t-\Delta t)/(2\Delta t)}{\breve{\gamma}(t-\Delta t)},$$

$$\breve{\theta}_0(t) = \frac{1}{(2\Delta t)\breve{\gamma}(t-\Delta t)},$$

$$\breve{\theta}_1(t) = -\frac{\dot{k}(t-\Delta t)}{k(t-\Delta t)\breve{\gamma}(t-\Delta t)},$$

$$\breve{\theta}_2(t) = \frac{-1}{(2\Delta t)\breve{\gamma}(t-\Delta t)},$$

$$\breve{\gamma}(t-\Delta t) = \frac{m(t-\Delta t)}{(\Delta t)^2} + \frac{\breve{c}(t-\Delta t)}{(2\Delta t)},$$

$$\breve{c}(t) = \dot{m}(t) + c(t) - \frac{m(t)\dot{k}(t)}{k(t)},$$

$$\breve{k}(t) = k(t) + \dot{c}(t) - \frac{c(t)\dot{k}(t)}{k(t)} \tag{30}$$

Similarly, if acceleration responses are employed, one can establish

$$a(t) = \tilde{\phi}_1(t)a(t-\Delta t) + \tilde{\phi}_2(t)a(t-2\Delta t) + \tilde{\theta}_0(t)f(t) + \tilde{\theta}_1(t)f(t-\Delta t) + \tilde{\theta}_2(t)f(t-2\Delta t) \tag{31}$$

where $a(t)$ denotes acceleration responses, and

$$\tilde{\phi}_1(t) = -\frac{\tilde{k}(t-\Delta t) - 2m(t-\Delta t)/(\Delta t)^2}{\tilde{\gamma}(t-\Delta t)},$$

$$\tilde{\phi}_2(t) = -\frac{m(t-\Delta t)/(\Delta t)^2 - \tilde{c}(t-\Delta t)/(2\Delta t)}{\tilde{\gamma}(t-\Delta t)},$$

$$\tilde{\theta}_0(t) = \frac{1}{\tilde{\gamma}(t-\Delta t)}\left(\frac{1}{(\Delta t)^2} - \frac{\dot{k}(t-\Delta t)}{(2\Delta t)k(t-\Delta t)} - \frac{\dot{\breve{k}}(t-\Delta t)}{(2\Delta t)\breve{k}(t-\Delta t)}\right),$$

$$\bar{\theta}_1(t) = \frac{1}{\tilde{\gamma}(t-\Delta t)} \times \left(\frac{-2}{(\Delta t)^2} - \frac{k(t-\Delta t)\ddot{k}(t-\Delta t) - \left(\dot{k}(t-\Delta t)\right)^2}{\left(k(t-\Delta t)\right)^2} + \frac{\dot{k}(t-\Delta t)\dot{\breve{k}}(t-\Delta t)}{k(t-\Delta t)\breve{k}(t-\Delta t)}\right),$$

$$\tilde{\theta}_2(t) = \frac{1}{\tilde{\gamma}(t-\Delta t)}\left(\frac{1}{(\Delta t)^2}\frac{\dot{k}(t-\Delta t)}{(2\Delta t)k(t-\Delta t)} + \frac{\dot{\breve{k}}(t-\Delta t)}{(2\Delta t)\breve{k}(t-\Delta t)}\right),$$

$$\tilde{\gamma}(t-\Delta t) = \frac{m(t-\Delta t)}{(\Delta t)^2} + \frac{\tilde{c}(t-\Delta t)}{(2\Delta t)},$$

$$\tilde{c}(t) = \dot{m}(t) + \breve{c}(t) - \frac{m(t)\dot{\breve{k}}(t)}{\breve{k}(t)},$$

$$\tilde{k}(t) = \breve{k}(t) + \dot{\breve{c}}(t) - \frac{\breve{c}(t)\dot{\breve{k}}(t)}{\breve{k}(t)} \tag{32}$$

Equations (25), (29), and (31) indicate the equivalence between the discrete form of the equation of motion and TVARX model when noise variable $a_n(t)$ does not exist. Accordingly, when displacement responses are used, (I, J) in Equation (3) should be (2, 1) and $\theta_0(t) = 0$. When velocity or acceleration responses are used, (I, J) in Equation (3) should be (2, 2).

As the relationship between Equations (1) and (3) is now known, attention now turns to the evaluation of instantaneous modal parameters. When displacement responses are used to establish the TVARX model,

Equation (25) should be obtained theoretically. Then, the roots of Equation (21) are

$$\lambda_{1,2} = c_1 \pm i d_1 \tag{33}$$

where

$$c_1 = \frac{2m(t-\Delta t) - (\Delta t)^2 k(t-\Delta t)}{2m(t-\Delta t) + c(t-\Delta t)\Delta t},$$

$$d_1 = \frac{\Delta t\left[4m(t-\Delta t)k(t-\Delta t) - (\Delta t)^2 k^2(t-\Delta t) + c^2(t-\Delta t)\right]^{1/2}}{2m(t-\Delta t) + c(t-\Delta t)\Delta t} \tag{34}$$

The argument, $t - \Delta t$, in functions m, c, and k, is not shown in the following equations to simplify the expressions. Substituting Equation (34) into Equation (23) yields

$$\alpha_1 = \frac{1}{2\Delta t}\ln\left(\frac{2m - c\Delta t}{2m + c\Delta t}\right) \quad \text{and}$$

$$\beta_1 = \frac{1}{\Delta t}\tan^{-1}\left[\frac{\Delta t\left[4mk - k^2(\Delta t)^2 + c^2\right]^{1/2}}{2m - k(\Delta t)^2}\right] \tag{35}$$

The Taylor expressions of α_1 and β_1 given by Equation (35) are

$$\alpha_1 = \left\{-\frac{2\pi\xi}{T} + O\left(\frac{\Delta t}{T}\right)^2\right\}$$

and

$$\beta_1 = \left\{\left(\frac{(2\pi)[1-\xi^2]^{\frac{1}{2}}}{T}\right) + \frac{1}{3!T}\left(\frac{3\pi T^2}{2[1-\xi^2]^{\frac{1}{2}}} + 24\pi^3[1-\xi^2]^{\frac{1}{2}} - 16\pi^3[1-\xi^2]^{\frac{3}{2}}\right)\left(\frac{\Delta t}{T}\right)^2 + O\left(\frac{\Delta t}{T}\right)^4\right\} \tag{36}$$

where $T = 2\pi\sqrt{m/k}$, which is the instantaneous period, and $O((\Delta t/T)^n)$ are terms with an order in $(\Delta t/T)$ higher than (or equal to) n. It is well known that $(\Delta t/T)$ must be sufficiently small to have an accurate finite difference presentation for the equation of motion. Accordingly, when $(\Delta t/T)$ approaches zero, Equation (36) can be simplified as

$$\alpha_1 = -\frac{2\pi\xi}{T} \quad \text{and} \quad \beta_1 = \frac{2\pi}{T}(1-\xi^2)^{1/2} \tag{37}$$

Substituting Equation (37) into Equation (22) yields

$$\omega_1 = \frac{2\pi}{T} = \sqrt{\frac{k}{m}} \quad \text{and} \quad \xi_1 = \xi = \frac{c}{2\sqrt{km}} \tag{38}$$

Similarly, one obtains the following results from the coefficient functions of the TVARX model established using velocity or acceleration responses:

$$\omega_{1v} = \sqrt{\frac{\breve{k}}{m}} \quad \text{and} \quad \xi_{1v} = \frac{\breve{c}}{2\sqrt{\breve{k}m}} \tag{39}$$

or

$$\omega_{1a} = \sqrt{\frac{\tilde{k}}{m}} \quad \text{and} \quad \xi_{1a} = \frac{\tilde{c}}{2\sqrt{\tilde{k}m}} \tag{40}$$

where subscripts v and a denote the computational results obtained from velocity and acceleration responses, respectively. Accordingly, ω_{1v}, ω_{1a}, ξ_{1v}, and ξ_{1a} obtained from the TVARX model can differ significantly from the true instantaneous modal parameters of a structural system under consideration. Comparison of Equations (1) and (27) reveals that ω_{1v} and ξ_{1v} are equal to the true instantaneous modal parameters at $t = \hat{t}$ when $\dot{m}(\hat{t})$, $\dot{c}(\hat{t})$, and $\dot{k}(\hat{t})$ equal zero.

4 NUMERICAL VERIFICATION

Numerical simulation responses were processed to demonstrate the feasibility of the proposed procedure. The Runge–Kutta method was applied to determine the needed dynamic responses of Equation (1), with a time increment (Δt) equal to 0.001 second. Consider a system with a single degree of freedom defined by Equation (41) subjected to the base excitation ($a_g(t)$) (Figure 1),

$$\ddot{x}(t) + 2\xi(t)\omega_n(t)\dot{x}(t) + \omega_n(t)^2 x(t) = -a_g(t) \tag{41}$$

Two instantaneous modal parameter types are considered here and defined as follows:

Type I: Slowly varying system

$$\omega_n(t) = 2\pi\left(1.5 - 0.5\sin\left(\frac{2\pi}{60}t\right)\right),$$

$$\xi(t) = 4 + 2\sin\left(\frac{2\pi}{60}t\right), \quad 0 \le t \le 30 \tag{42}$$

Type II: Periodically varying system

$$\omega_n(t) = 2\pi\left(1.0 - 0.5\sin\left(\frac{2\pi}{10}t\right)\right),$$

$$\xi(t) = 5 + 2.5\sin\left(\frac{2\pi}{10}t\right), \quad 0 \le t \le 30 \tag{43}$$

The instantaneous modal parameters defined by Equation (43) vary with time much more rapidly than those defined by Equation (42). Displacement responses were processed in the following system identification. Figure 1 presents the time histories of displacement responses for slowly varying and periodically varying systems.

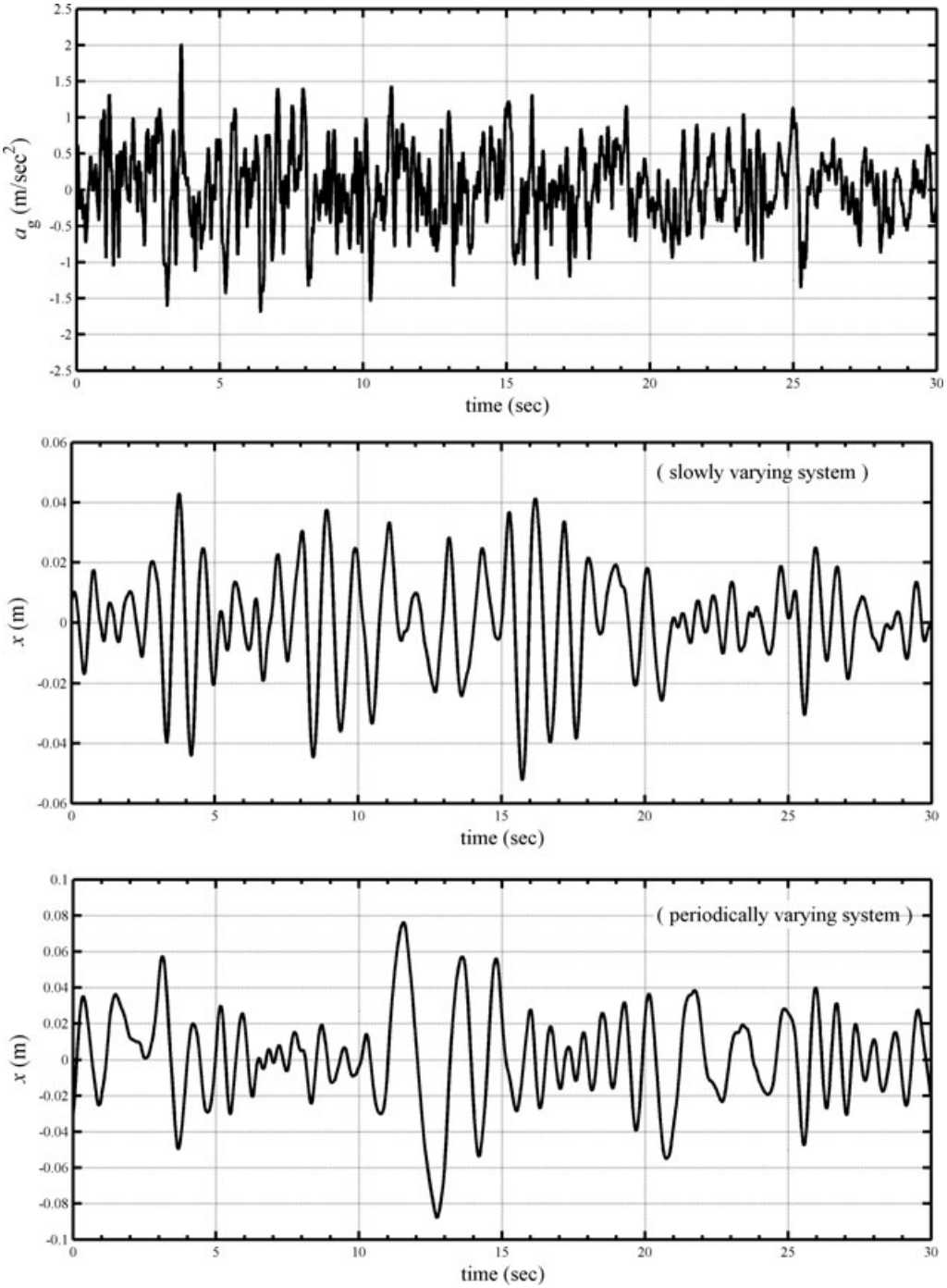

Fig. 1. Input acceleration and displacement responses.

The effects of noise and some parameters involved in the proposed procedure on determining instantaneous modal parameters are investigated thoroughly. The parameters considered are the support of the weight function (d in Equation (20)), the order of polynomial basis (N_i and $\bar{N}_j$ in Equation (4)), and number of nodal points ($\bar{l}_i$ in Equation (5)). For simplicity, N_i and $\bar{N}_j$ are set to equal $\bar{N}$ for all i and j; $\bar{l}_i$ is also set to equal $\hat{l}$ for all i.

4.1 Parametric studies

The TVARX(2, 1) model is used in this section. After setting the desired parameters (i.e., d, $\bar{N}$, and $\hat{l}$), the

Table 1
Means and variances of relative errors of identified instantaneous modal parameters

			Slowly varying system				*Periodically varying system*			
			$\sigma(\%)$		$\mu(\%)$		$\sigma(\%)$		$\mu(\%)$	
$\hat{l}$	$\bar{N}$	d	f_n	ξ	f_n	ξ	f_n	ξ	f_n	ξ
20	0	2	0.645	1.566	1.070	2.187	6.721	11.81	8.091	20.64
		4	0.077	0.245	0.141	0.301	1.623	3.224	2.018	4.305
		6	0.014	0.022	0.011	0.022	0.469	1.401	0.493	1.406
	1	2	0.033	0.104	0.039	0.120	4.145	5.115	2.848	6.553
		4	0.011	0.033	0.018	0.047	1.381	2.062	1.462	2.365
		6	0.001	0.006	0.007	0.014	0.524	1.587	0.531	1.524
	2	2	0.053	2.907	0.037	1.428	1.051	4.293	1.513	5.427
		4	0.003	0.008	0.006	0.013	0.770	3.048	1.096	3.655
		6	0.001	0.004	0.007	0.013	0.446	1.485	0.652	2.024
	3	2	37.57	38.08	28.57	65.52	34.71	63.27	29.53	102.2
		4	0.001	0.005	0.007	0.014	0.562	1.736	0.880	2.501
		6	0.001	0.005	0.007	0.014	0.414	1.100	0.605	1.832
35	0	2	0.107	0.642	0.171	0.705	1.069	11.59	1.447	10.15
		4	0.005	0.029	0.008	0.024	0.104	0.232	0.083	0.177
		6	0.002	0.009	0.007	0.014	0.080	0.136	0.068	0.153
	1	2	0.007	0.034	0.011	0.043	0.594	1.959	0.601	2.173
		4	0.001	0.005	0.007	0.014	0.050	0.108	0.059	0.108
		6	0.001	0.005	0.007	0.014	0.023	0.035	0.047	0.067
	2	2	0.001	0.008	0.007	0.016	0.214	2.385	0.332	2.480
		4	0.001	0.005	0.007	0.014	0.026	0.106	0.049	0.106
		6	0.001	0.005	0.007	0.014	0.032	0.076	0.054	0.087
	3	2	0.001	0.025	0.007	0.021	0.108	0.675	0.117	0.580
		4	0.001	0.005	0.007	0.014	0.033	0.100	0.052	0.096
		6	0.001	0.005	0.007	0.014	0.024	0.037	0.046	0.063

instantaneous modal parameters at any instant time $t = t_i$ can be determined using the proposed procedure. The relative error of identified instantaneous modal parameters at $t = t_i$ is defined as

$$\frac{\left|\rho_{\text{id}}(t_i) - \rho_{\text{true}}(t_i)\right|}{\rho_{\text{true}}(t_i)} \times 100\% \tag{44}$$

where ρ_{true} and ρ_{id} are the true and identified instantaneous natural frequency (f_n) or damping ratio (ξ), respectively. Table 1 summarizes the means (μ) and variances (σ) of relative errors of instantaneous parameters identified using different numbers of nodal points ($\hat{l} = 20$ and 35), various orders of the polynomial basis ($\bar{N} = 0, 1, 2,$ and 3), and different supports of the weight function ($d = 2$, 4, and 6 seconds). Figures 2 and 3 display the means of relative errors of the identified instantaneous modal parameters acquired using different numbers of nodal points for slowly varying and periodically varying systems, respectively.

Table 1 and Figures 2 and 3 show several interesting facts. Using the parameter values given in Table 1 yields accurately identified f_n or ξ, except for some results obtained using $d = 2$. The instantaneous modal parameters identified using $d = 4$ or 6 are considerably more accurate than those obtained using $d = 2$, especially in the cases of small $\hat{l}$ (i.e., $\hat{l} = 20$) and large $\bar{N}$ (i.e., $\bar{N} = 3$). Figures 2 and 3 show that using larger $\hat{l}$ yields more accurate results of identification when $d = 4$ or 6 and $\bar{N} = 0, 1, 2,$ or 3 are utilized. The proposed approach does not need polynomial basis functions with high orders. These facts demonstrate the important features of the proposed procedure.

Figures 4 and 5 present the comparison of the identified instantaneous modal parameters with true values for slowly varying and periodically varying systems, respectively. The instantaneous modal parameters were identified using $d = 4$, $\bar{N} = 2$, and $\hat{l} = 30$ in the proposed approach. A recursive technique with a constant forgetting factor equal to 0.95 (Ljung, 1987) was also applied to determine the instantaneous modal parameters shown in Figures 4 and 5. The results of the proposed approach are highly accurate, with the relative errors much less than 1%, and substantially better than those obtained using the recursive technique. When the periodically varying system is considered, the recursive

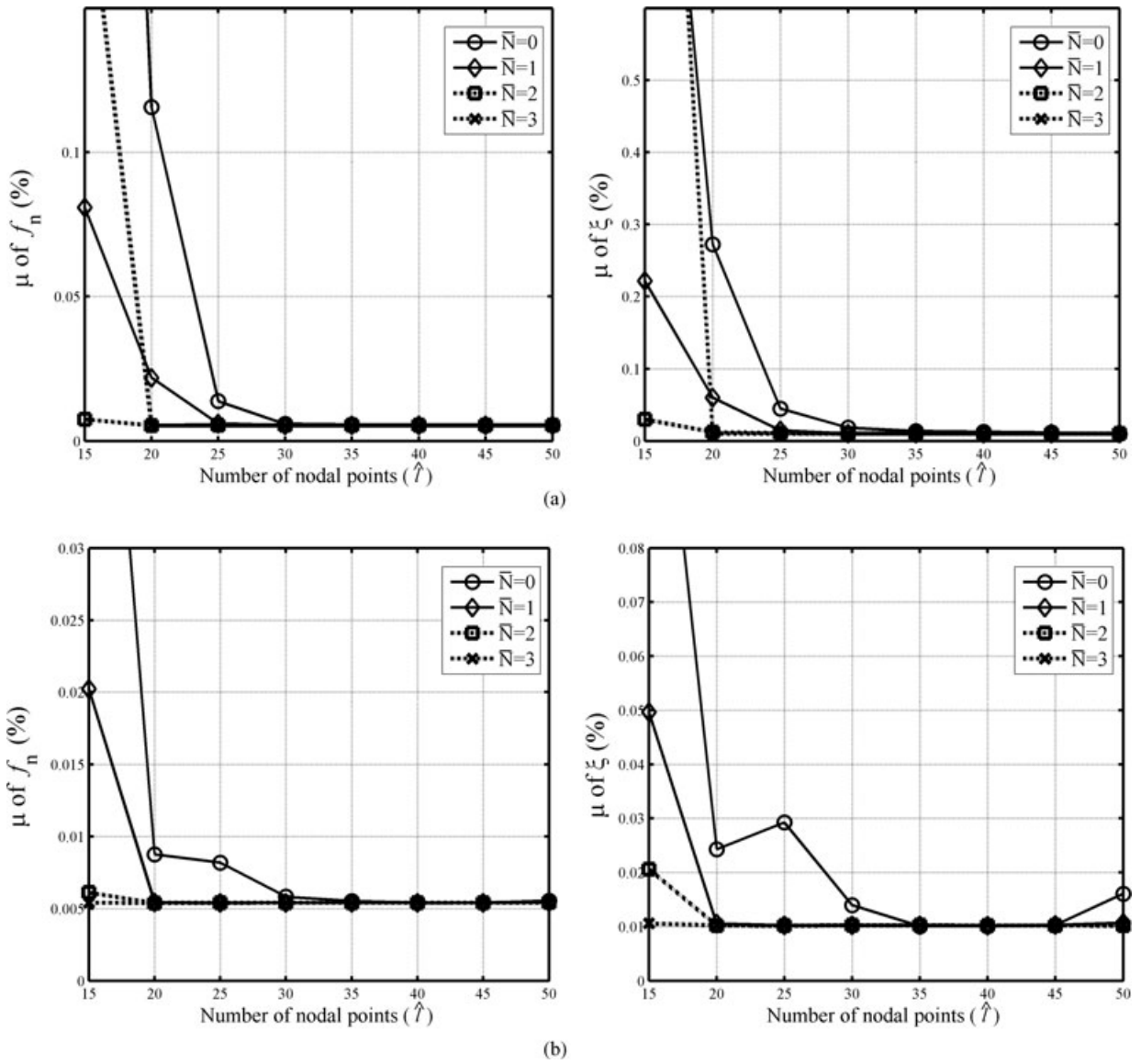

Fig. 2. Means of relative errors of identified f_n and ξ varying with $\hat{l}$ for a slowly varying system: (a) $d = 4$ seconds; (b) $d = 6$ seconds.

technique has very limited capability of identifying the instantaneous damping ratios varying with time.

Figure 6 depicts the instantaneous parameters for the periodically varying system identified using a traditional basis function expansion technique and a weighted basis function approach (Niedźwiecki, 2000) whose results are denoted by "BF" and "WBF," respectively. The "BF" results were obtained using 20 polynomial basis functions ($\{1, t, t^2, \ldots, t^{19}\}$), although the "WBF" results were determined using the same polynomial basis functions ($\{1, t, t^2\}$) and weighting function (Equation (20) with $d = 4$) as those employed to obtain the results denoted by "proposed" in Figure 5. Comparison of the results in Figures 5 and 6 reveals that the proposed approach gives much more accurate results than the traditional basis function expansion technique and the approach of Niedźwiecki (2000) do. Notably, using more polynomial basis functions in the traditional basis function expansion approach does not significantly improve the accuracy of results. An Intel®-based PC with 2.40-GHz CPU was used to calculate all the numerical results shown here. It took 28.2 and 54.3 seconds of CPU time to obtain the results utilizing the present approach and the approach of Niedźwiecki (2000), respectively.

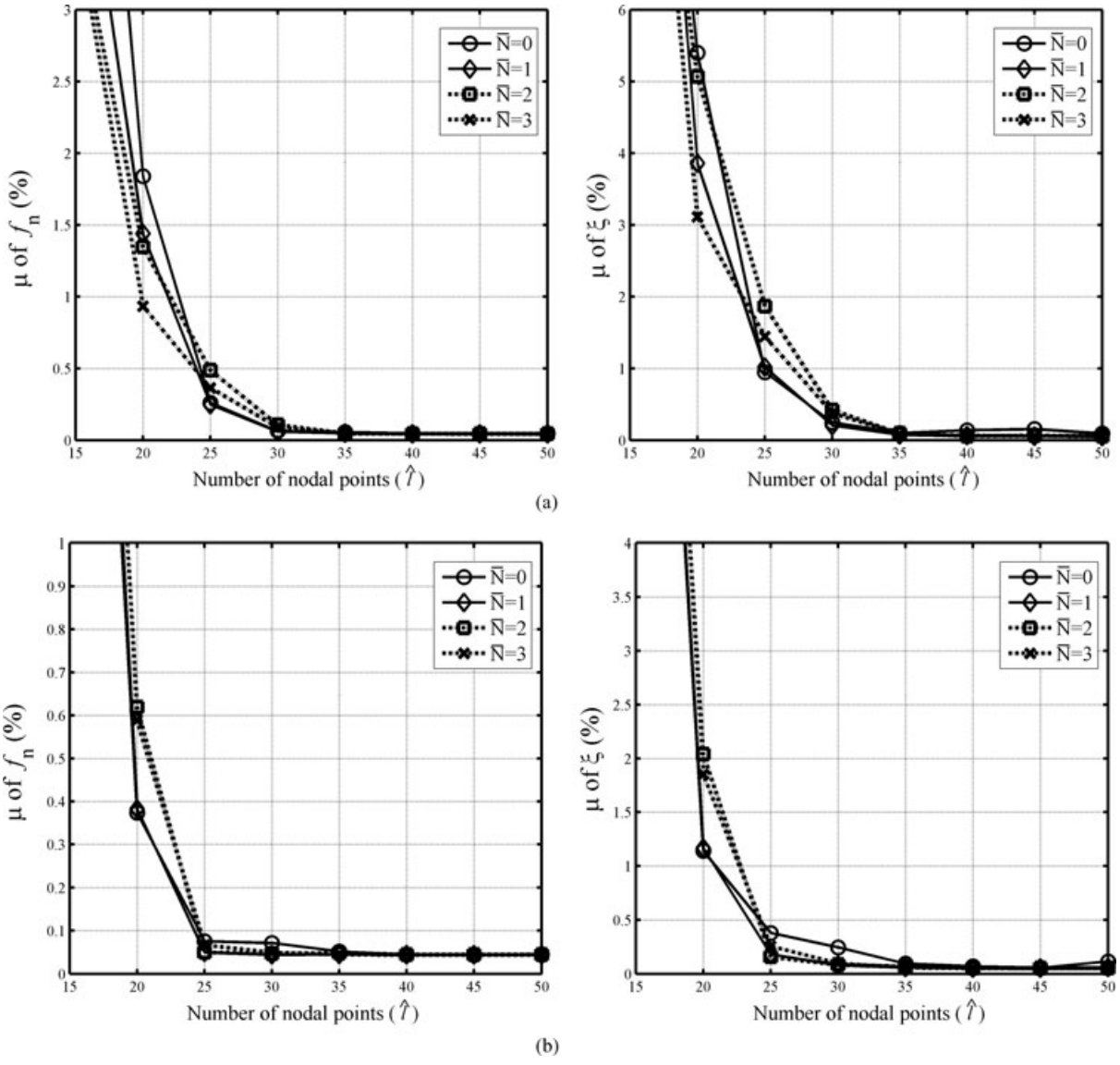

Fig. 3. Means of relative errors of identified f_n and ξ varying with $\hat{l}$ for a periodically varying system: (a) $d = 4$ seconds; (b) $d = 6$ seconds.

4.2 Effects of noise and selection of a suitable order of the TVARX model

Noise is always found in measured data. White noise was added to numerical simulation displacement responses and input acceleration to assess the effect of noise on the accuracy of instantaneous modal parameters identified using the proposed approach. The variance of the noise-to-signal ratio is set at 5%. Similar to processing noisy data for a time-invariant system, the order of the TVARX model must increase to accommodate noise.

Figures 7 and 8 depict the means of relative errors of identified instantaneous modal parameters varying with the orders of the TVARX model for the slowly varying and periodically varying systems, respectively. For simplicity, I is set equal to J in the TVARX(I, J) model in the following computations. The instantaneous modal parameters were obtained using $\bar{N} = 2$, $d = 4$ or 6, and $\hat{l} = 25, 30,$ or 35. The means of relative errors of identified instantaneous modal parameters generally decrease as I and J increase. As expected, noise significantly impacts the accuracy of identified instantaneous modal parameters, especially when identifying instantaneous modal damping ratios. The accuracy of the identified results (Figures 7 and 8) using large I and J is not as good as those (Table 1) for data without noise. Nevertheless, Figures 7 and 8 show that using large I and J can yield

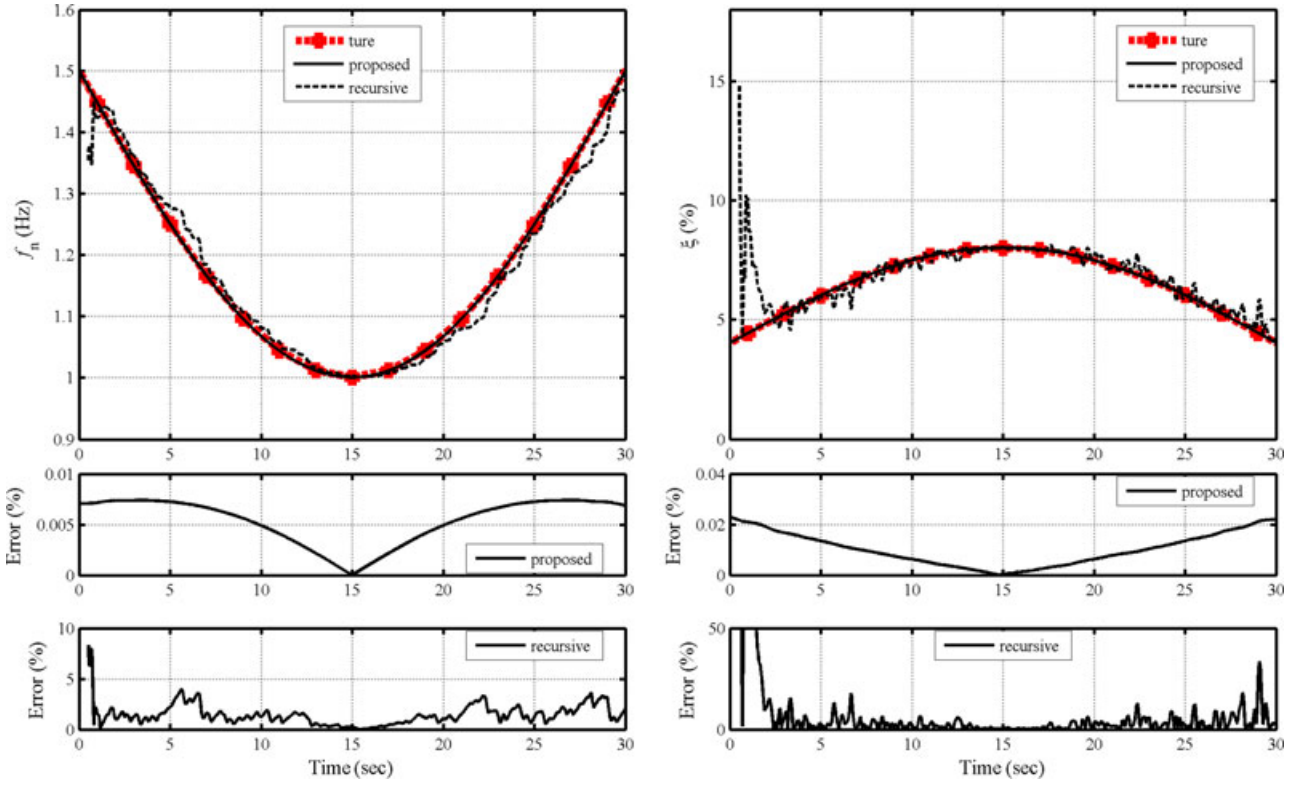

Fig. 4. Identified f_n and ξ for a slowly varying system.

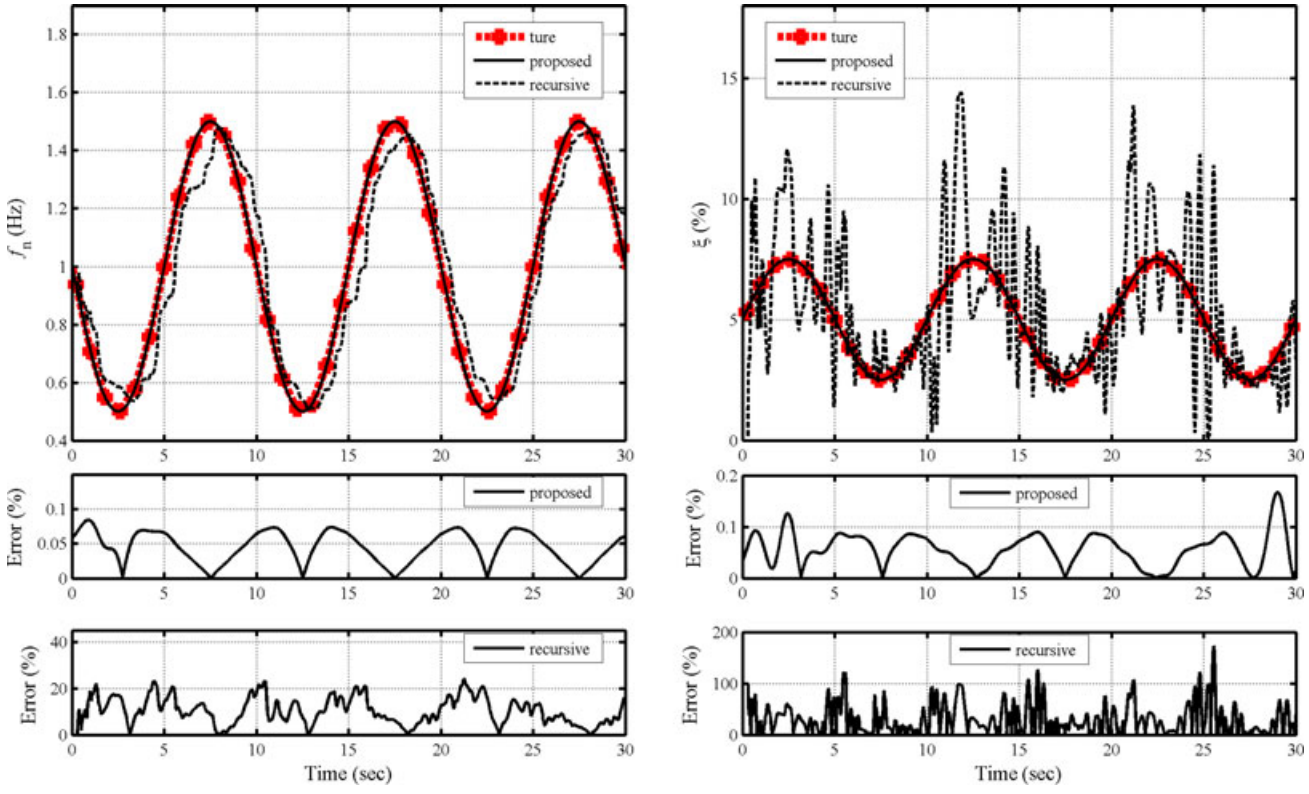

Fig. 5. Identified f_n and ξ for a periodically varying system.

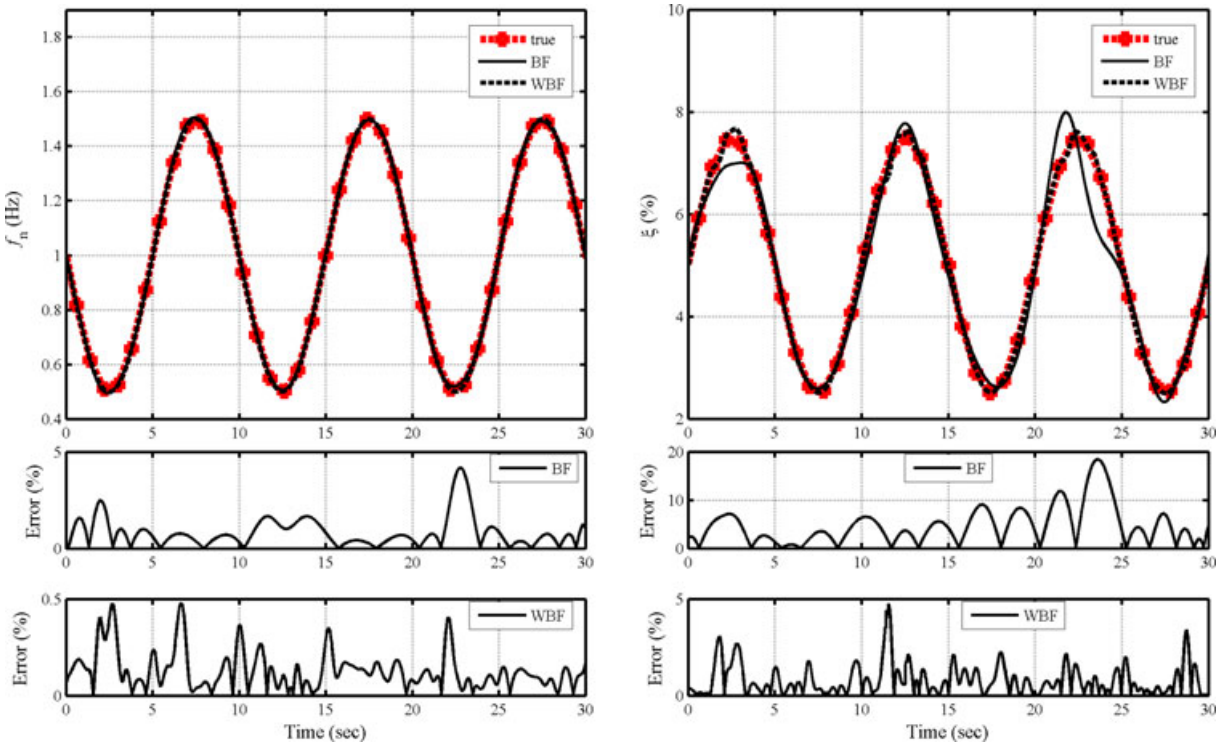

Fig. 6. Identified f_n and ξ for a periodically varying system by two existing approaches.

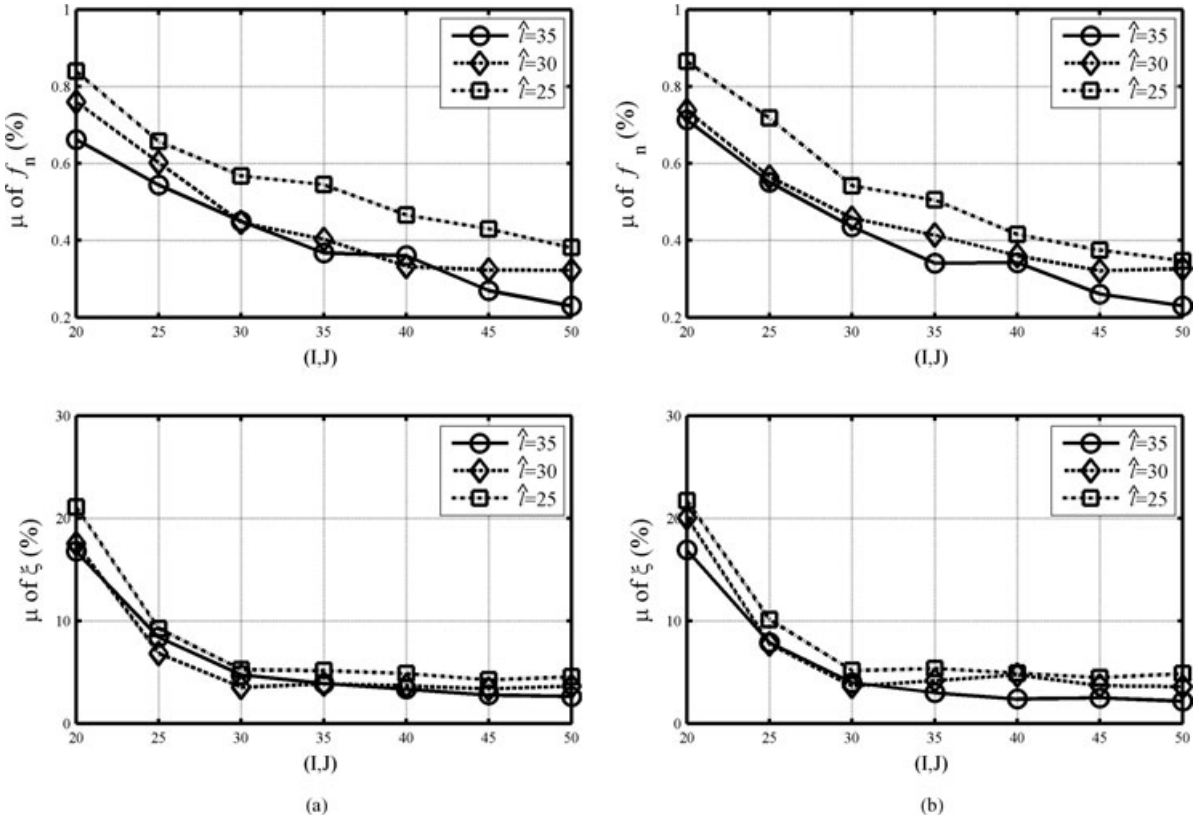

Fig. 7. Variation of means of relative errors of identified f_n and ξ with the orders of the TVARX model for a slowly varying system: (a) $d = 4$ seconds; (b) $d = 6$ seconds.

the means of relative errors of identified instantaneous modal frequencies and damping ratios less than 2% and 10%, respectively.

In real applications, the true instantaneous modal parameters are typically unknown. That is, one cannot estimate the means of relative errors of identified instantaneous modal parameters and decide the suitable order of the TVARX model. However, the Akaike information criterion (AIC) (Akaike, 1973), which was originally developed for a time-invariant system, is also often used to determine suitable I and J values in the TVRAX(I, J) model (Tsatsanis and Giannakis, 1993). The AIC is defined as

$$\mathrm{AIC} = N_T \ln V + 2N_d \tag{45}$$

where N_T is the number of data points used to construct the TVARX model, V is the mean square error of the one-step-ahead prediction from the TVARX model, and N_d is the total number of parameters in determining the coefficients of the TVARX model. In the proposed procedure, $N_\mathrm{d} = (I + J + 1) \times \hat{l}$ because each coefficient function in the TVARX(I, J) model is expanded using a series of functions with $\hat{l}$ parameters to be determined. Figure 9 shows the values of the AIC varying with orders of the TVARX model. These values of the AIC were obtained using $\bar{N} = 2$, $\hat{l} = 35$, and $d = 4$ or 6 seconds in the proposed approach. The value of the AIC generally decreases as I and J increase. When I and J are fixed, the values of the AIC determined using $d = 4$ seconds are significantly smaller than those obtained with $d = 6$ seconds. This trend is not consistent with that μ of f_n and ξ obtained using $d = 6$ may be smaller than those obtained with $d = 4$ (Figures 7 and 8). The reason for this inconsistency can be because the AIC value indicates level of agreement between the responses predicted by the TVARX(I, J) model and measured responses. When measured data contain noise, the TVARX model giving better prediction does not guarantee to yield more accurate identification of modal parameters.

An error index ($\bar{\mu}$) similar to the mean of relative errors of identified instantaneous modal parameters (Equation (44)) is proposed to supplement AIC when selecting a suitable order of the TVARX model. The error index is defined as

$$\bar{\mu}(I, J) = \frac{1}{n} \sum_{k=1}^{n} \left| \frac{\rho(I, J, t_k) - \rho(I-1, J-1, t_k)}{\rho(I, J, t_k)} \right| \tag{46}$$

where ρ (I, J, t_k) denotes the identified instantaneous natural frequency or damping ratio at $t = t_k$ obtained using the TVARX(I, J) model. When the TVARX(I, J) model results in highly accurate identification of instantaneous modal parameters, the value of $\bar{\mu}(I, J)$ will likely be very small. Figure 9 presents the $\bar{\mu}(I, J)$ of f_n and ξ varying with I and J, where f_n and ξ were obtained using $\bar{N} = 2$, $\hat{l} = 35$, and $d = 4$ or 6 seconds. The values of $\bar{\mu}(I, J)$ of f_n and ξ generally decrease as I and J increase.

The following two criteria are employed when choosing a suitable order of the TVARX model:

1. A suitable I and J must be chosen from a range of I and J in which $\bar{\mu}(I, J)$ changes with small fluctuations and must be less than the assigned threshold values that are case dependent.
2. A suitable I and J must be chosen from a range of I and J in which the value of the AIC changes with small fluctuations, or a suitable I and J yield the minimum value of the AIC in a broad range of I and J.

When $d = 4$ seconds was used, the TVARX(41, 41) and TVARX(50, 50) models were good models for the slowly varying system and periodically varying system, respectively (Figures 9 and 10). When $d = 6$ seconds was used, the TVARX(30, 30) and TVARX(40, 40) models were suitable for the slowly varying system and periodically varying system, respectively. Figures 11 and 12 display the instantaneous modal parameters identified using these TVARX models for slowly varying and periodically varying systems, respectively. Figures 11 and 12 also present a comparison of the identified instantaneous modal parameters with true values.

When $d = 4$ seconds was used, the TVARX(41, 41) model yielded the maximum relative errors of identified f_n and ξ of 2.2% and 30.2% for the slowly varying system, respectively. The TVARX(50, 50) model yields the maximum relative errors of f_n and ξ of 3.1% and 33.0%, respectively, for the periodically varying system. Nevertheless, most relative errors of ξ are less than 20%. When $d = 6$ was used, the TVARX(30, 30) model for the slowly varying system yielded 2.1% and 14.5% maximum relative errors for f_n and ξ, respectively. Most relative errors of ξ are less than 10%. The TVARX(40, 40) model for the periodically varying system generates the maximum relative errors of f_n and ξ of 3.9% and 22.6%, respectively. These identified f_n and ξ are sufficiently accurate for damage assessment of a structure because structural damage can be detected with confidence as its fundamental frequency shift exceeds 5% (Salawu, 1997).

Figure 13 displays the results identified using the weighted basis function approach proposed by Niedźwiecki (2000) to process the noisy data for the periodically varying system. The identified instantaneous f_n and ξ were obtained using the same polynomial basis functions ($\{1, t, t^2\}$) and weighting function (Equation (20) with $d = 6$) and TVARX model (TVARX(40, 40)) as those employed to obtain the

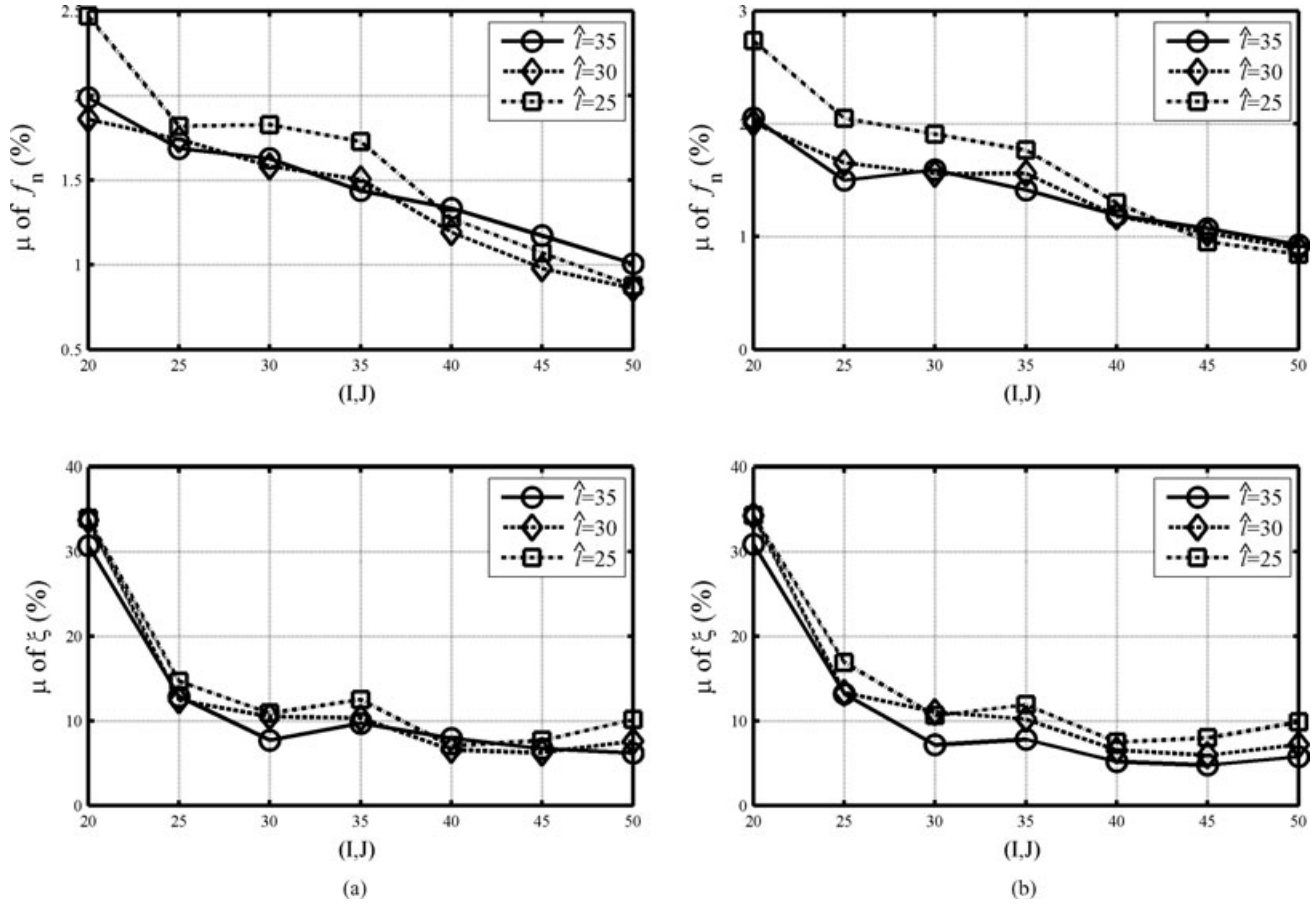

Fig. 8. Variation of means of relative errors of identified f_n and ξ with the orders of the TVARX model for a periodically varying system: (a) $d = 4$ seconds; (b) $d = 6$ seconds.

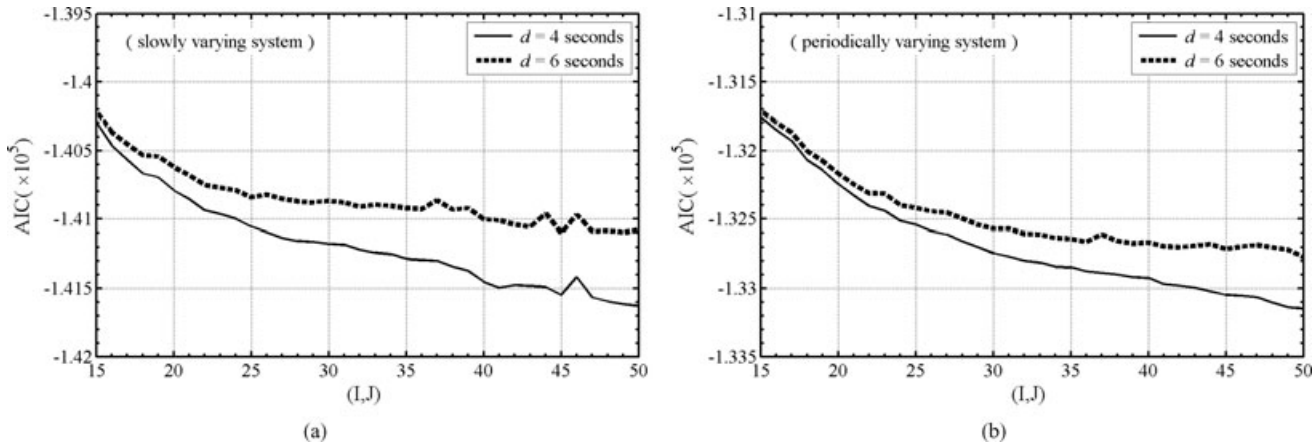

Fig. 9. Values of AIC varying with the orders of the TVARX model: (a) slowly varying system; (b) periodically varying system.

results denoted by "$d = 6$" in Figure 12. Comparing the results in Figure 13 with "$d = 6$" results in Figure 12 discovers that the present approach gives much better results than the weighted basis function approach in processing noisy data. Furthermore, it took 29.3 and 2,590.7 seconds of CPU time to obtain those results using the present approach and the weighted basis function approach, respectively. The present approach is substantially superior to the weighted basis function approach in accurately and efficiently

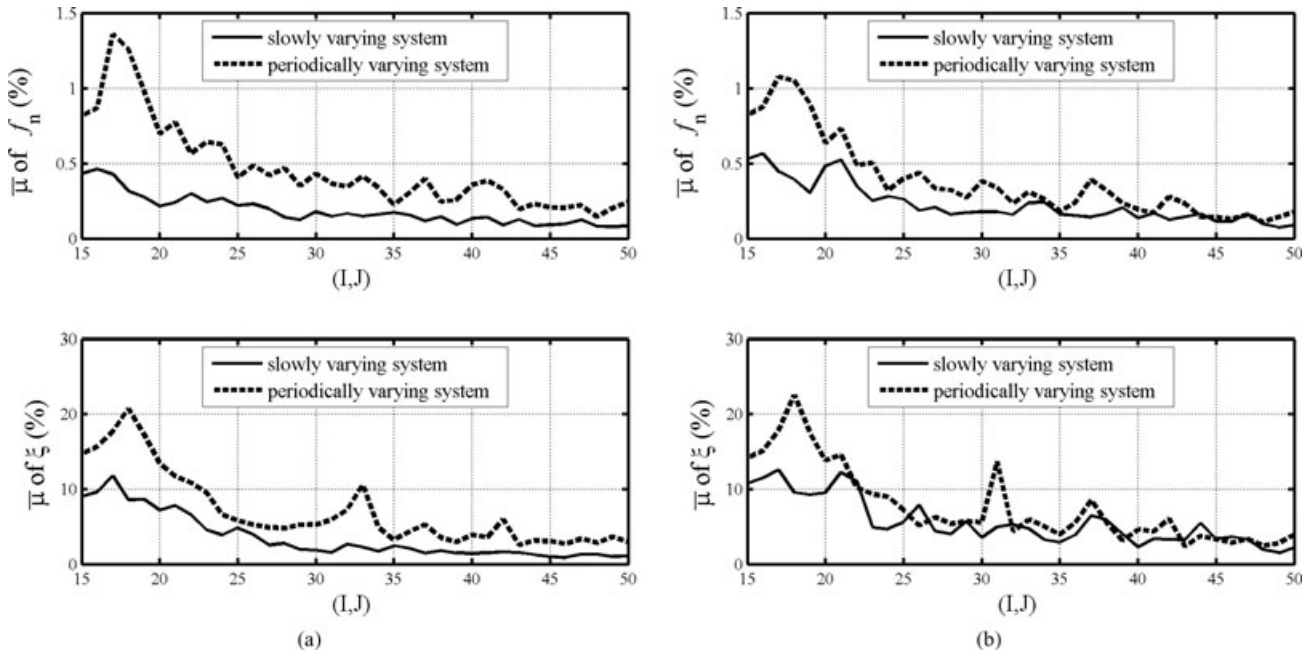

Fig. 10. The error index, $\bar{\mu}$, of f_n and ξ varying with the orders of the TVARX model: (a) $d = 4$ seconds; (b) $d = 6$ seconds.

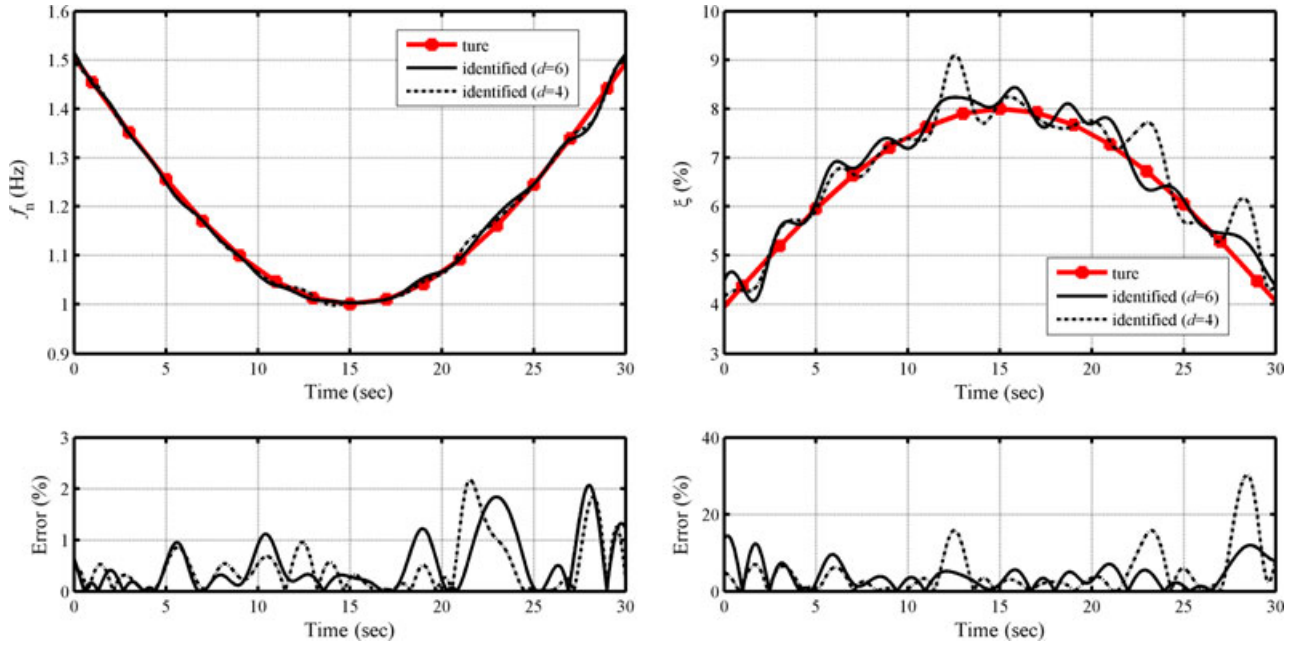

Fig. 11. Instantaneous modal parameters identified from noisy data for a slowly varying system.

estimating the instantaneous modal parameters of a structure.

5 APPLICATIONS TO MEASURED RESPONSES FROM SHAKING TABLE TESTS

Shaking table tests are vital to understanding the dynamic behaviors, especially nonlinear behaviors, of structural systems under earthquakes. The National Center for Research on Earthquake Engineering in Taiwan conducted a series of tests on reinforced concrete (RC) frames of two columns interconnected by a strong beam to investigate the dynamic behaviors of low-ductility RC columns and to understand their collapse mechanism. The details of testing programs are given by Wu et al. (2006). Figure 14 shows the

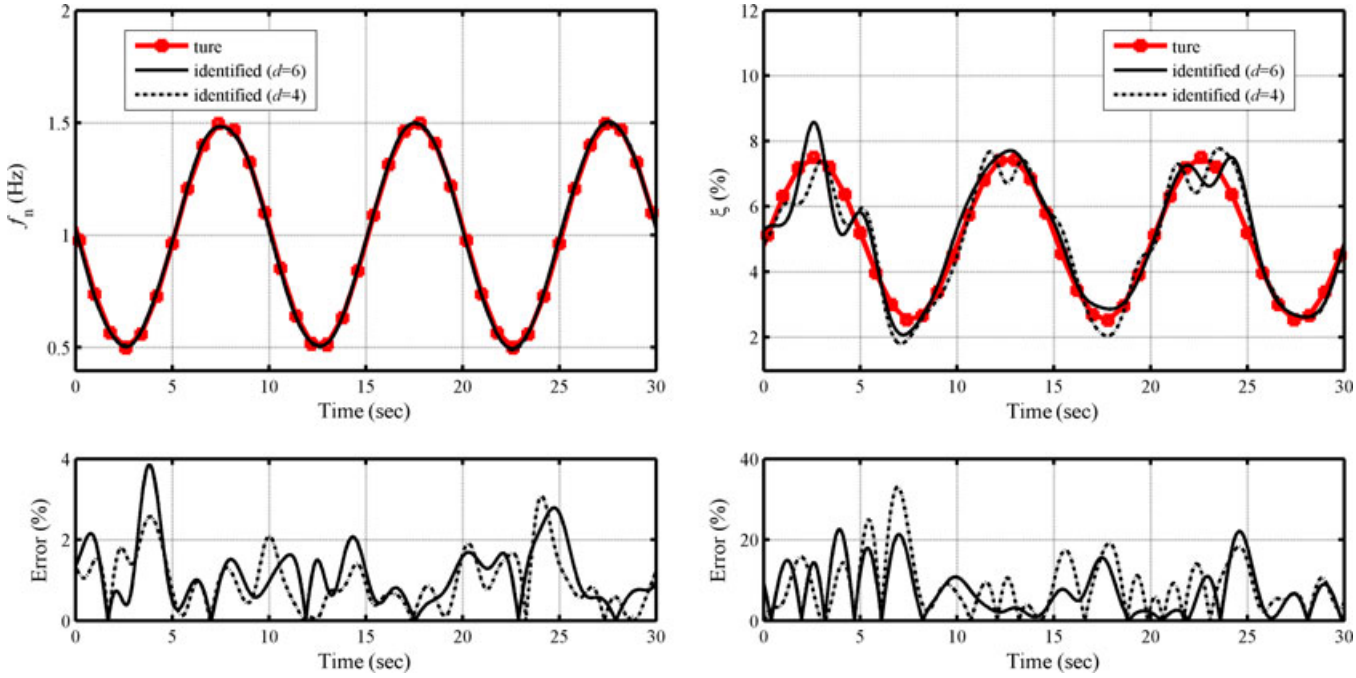

Fig. 12. Instantaneous modal parameters identified from noisy data for a periodically varying system.

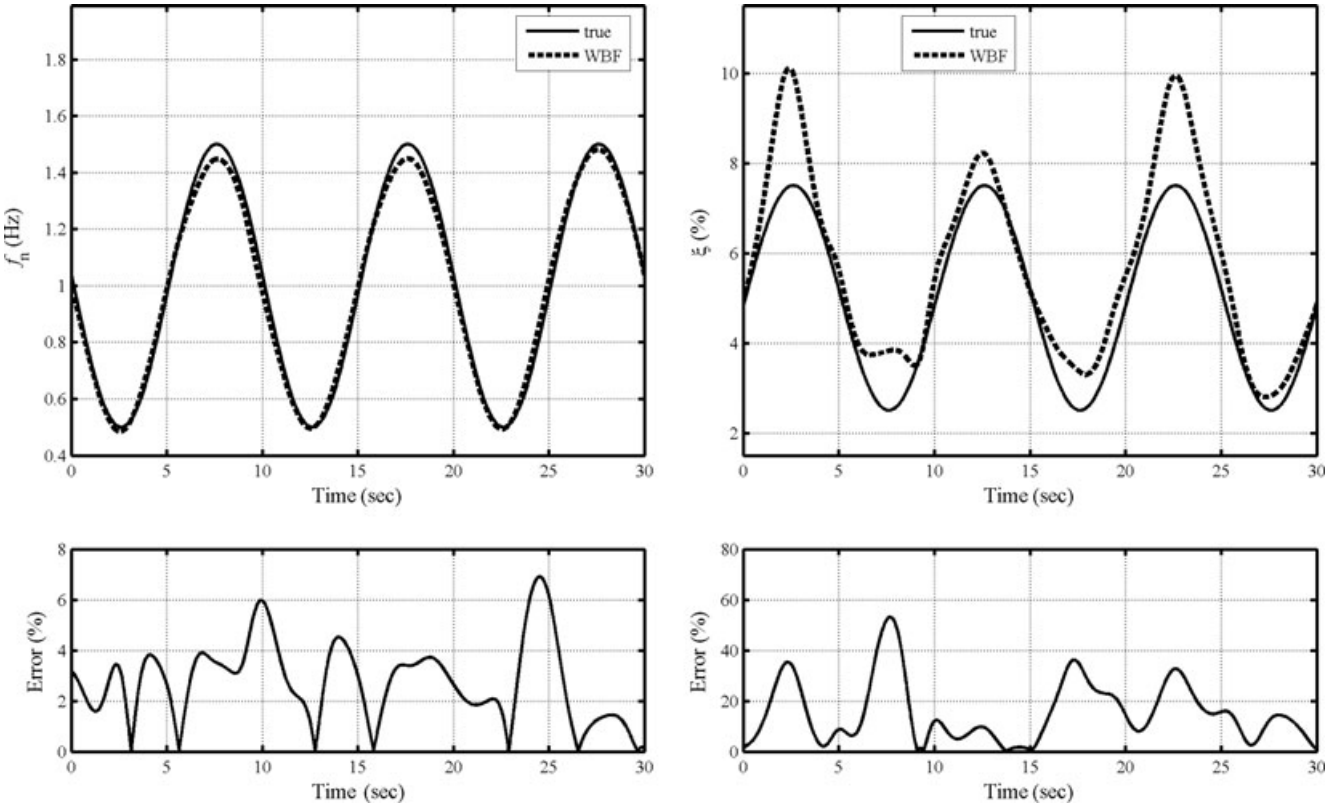

Fig. 13. Instantaneous modal parameters identified from noisy data by employing a weighted basis function approach.

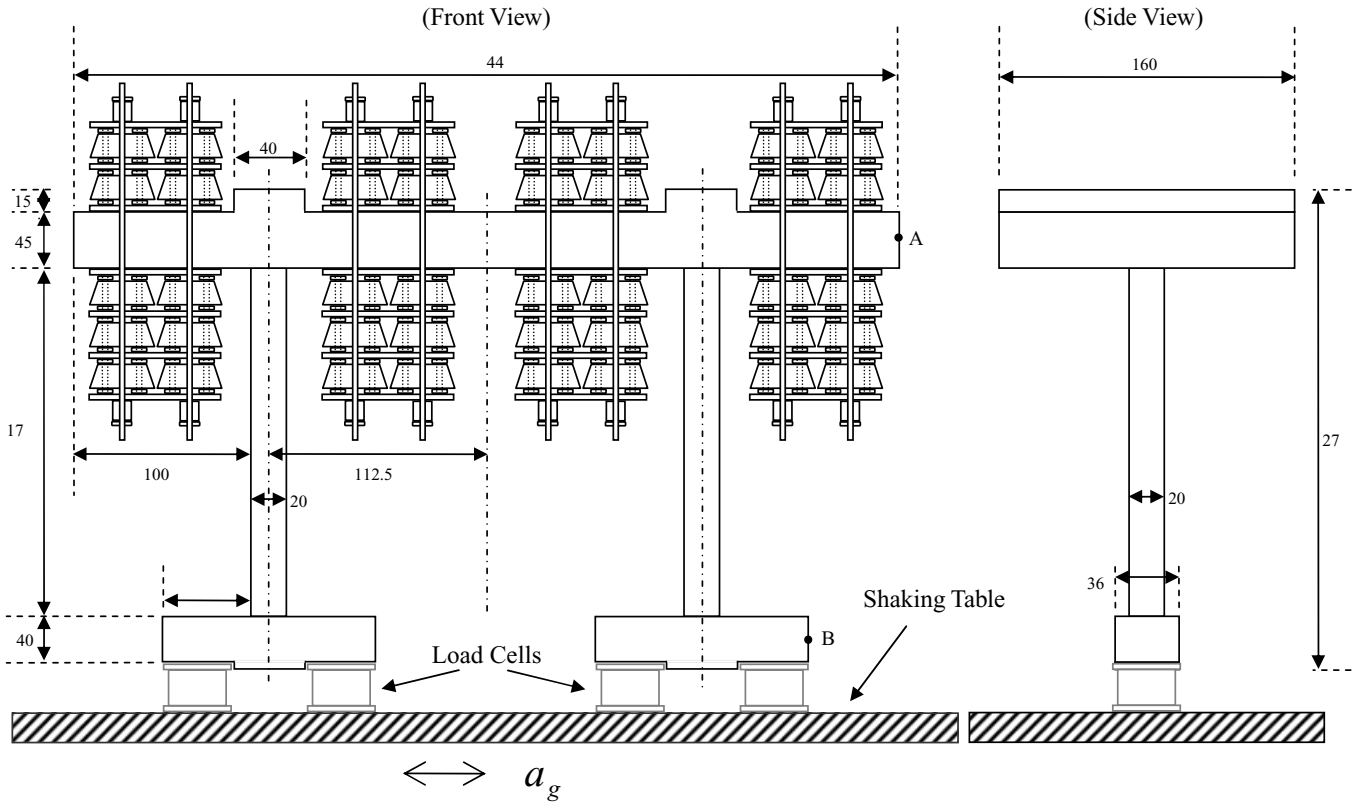

Fig. 14. A sketch of experiment setup.

dimensions of a typical frame and the test setup. In total, 21 tons of lead ballast was added to the beam (Figure 14) to simulate axial loads on first-story columns in a typical four-story RC building in Taiwan. Accelerometers and linear displacement transducers were installed at appropriate locations to measure acceleration and displacement responses of a specimen. Load cells were installed between the specimen and shaking table to measure base shear forces.

The specimen was subjected to a series of base excitation inputs; that is, it was first shaken under white noise input with small amplitude to estimate its modal parameters. The test is denoted as "before-damage" test because the specimen was not damaged. Then, the specimen was subjected to an earthquake input recorded during the 1999 Chi-Chi earthquake in Taiwan. Strong nonlinear behaviors were observed during this test, and columns near beam connection were damaged. The test is denoted as "during-earthquake" test. Finally, the specimen was shaken again with a low-level white noise input, which is denoted as "after-damage" test. Figure 15 shows the acceleration input and displacement response histories during these three tests. Displacement shown in Figure 15 is the horizontal relative displacement between A and B (Figure 14). Data were recorded at a sampling rate of 200 Hz. The Fourier spectra of these displacement responses are given in Figure 16.

The proposed identification procedure with $d = 6$, $\bar{N} = 2$, and $\hat{l} = 35$ was applied to process experimental data (Figure 15). By employing the criteria based on the AIC and $\bar{\mu}$ (discussed in the previous section), the TVARX(17, 17) and TVARX(34, 34) models were judged good models for processing data from the "before-damage" and "after-damage" tests, respectively, whereas the TVARX(36, 36) model could be appropriate for "during-earthquake" test data. The identified instantaneous modal parameters are shown in Figure 17.

As expected, small variations of instantaneous natural frequencies with time were observed for the cases with white noise input as no further damage occurred under such small input excitation forces. The identified instantaneous natural frequencies in the "before-damage" test are larger than those obtained from the "after-damage" test; the trend is opposite for the identified instantaneous modal damping ratios. The instantaneous natural frequencies in the "before-damage" test are 2.33–2.45 Hz, although those from the "after-damage" test are 1.57–1.66 Hz. These identified

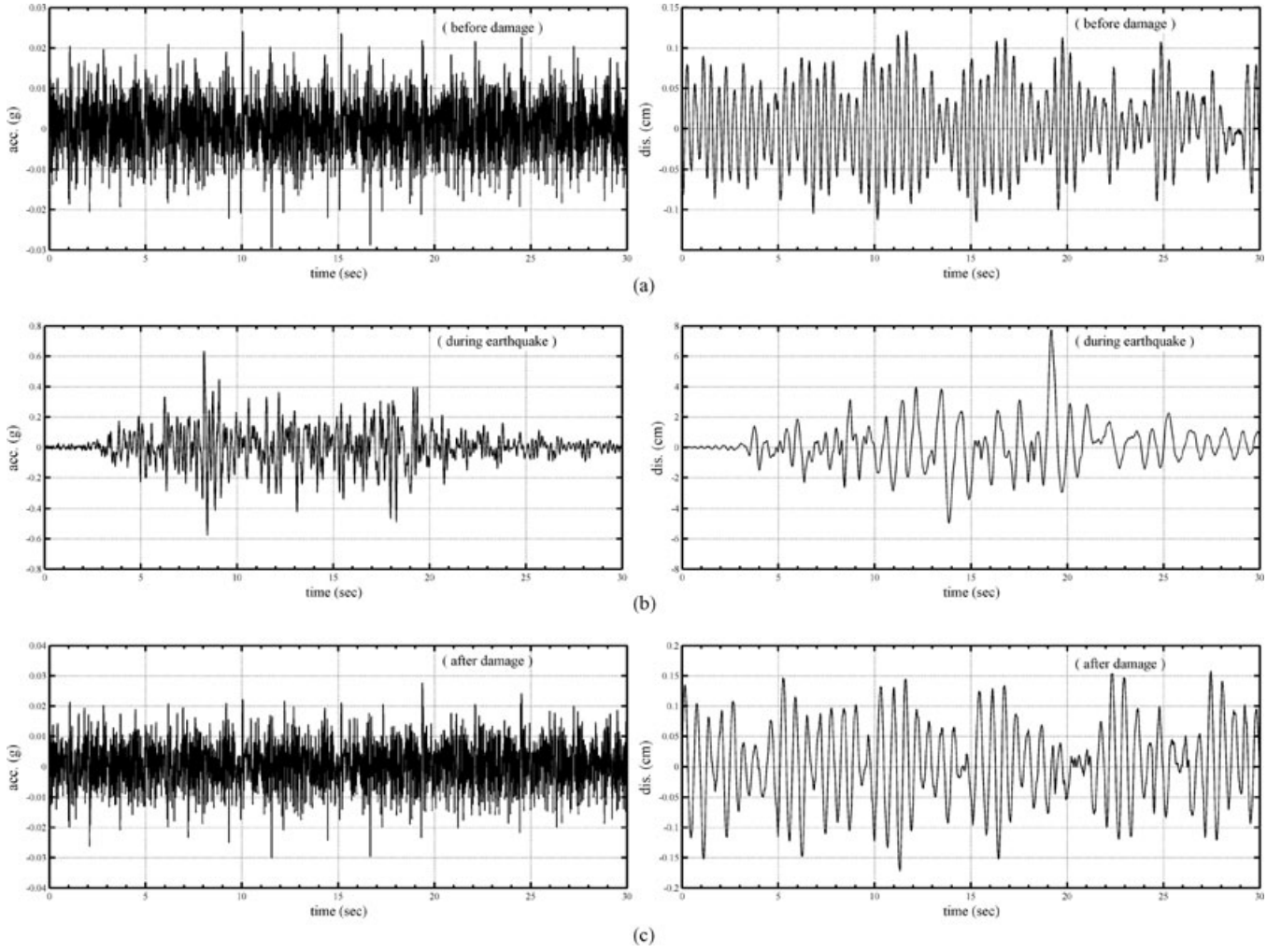

Fig. 15. The input acceleration and response histories from shaking table tests: (a) before damage; (b) during earthquake; (c) after damage.

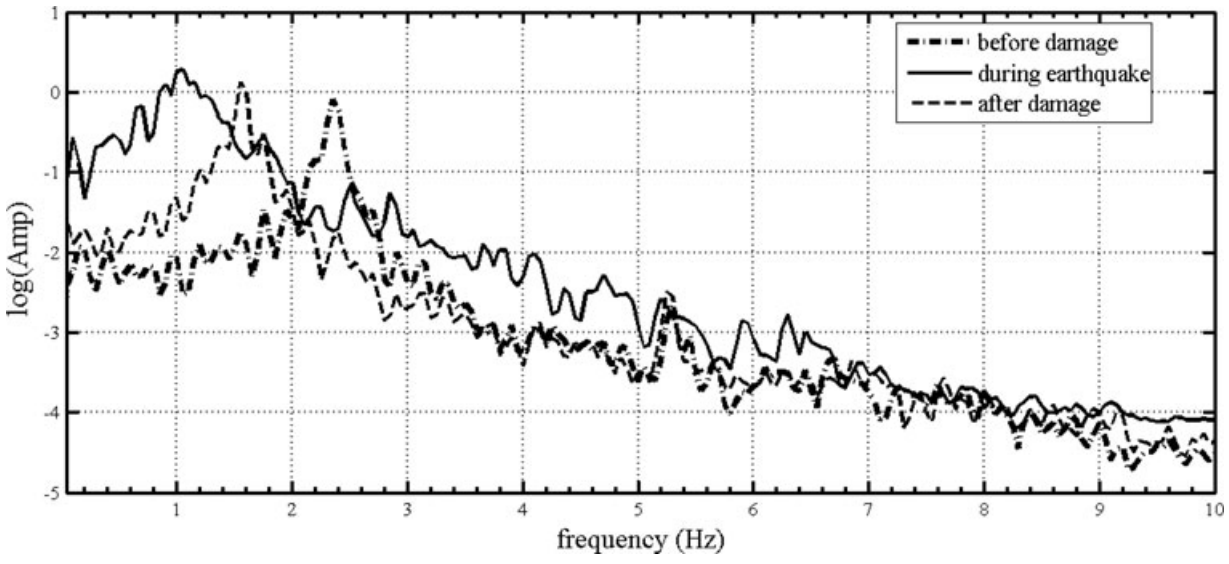

Fig. 16. Fourier spectra for displacement responses.

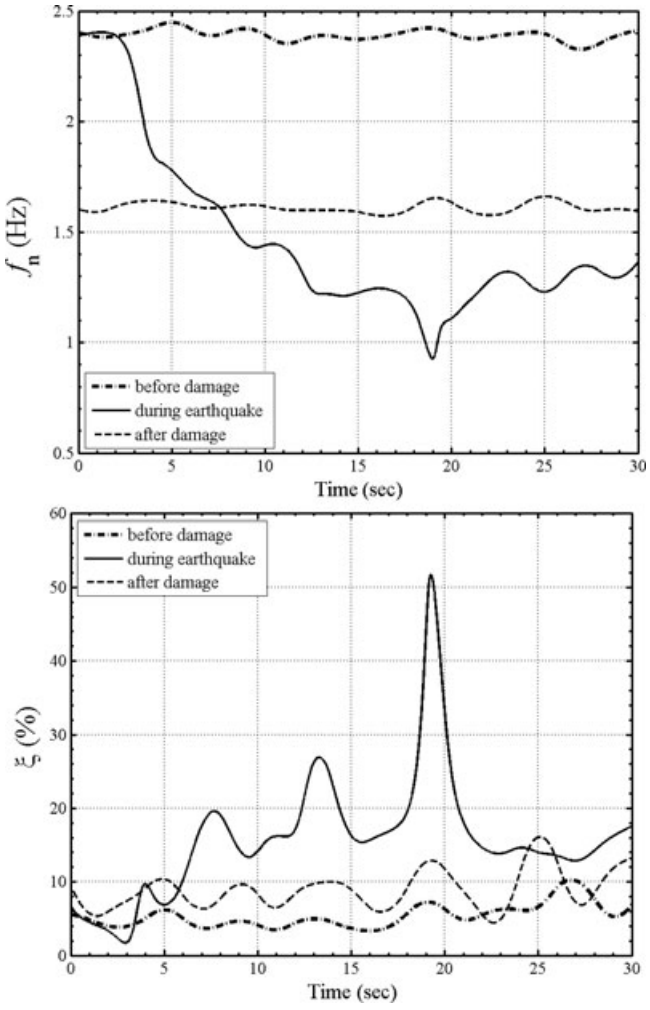

Fig. 17. Instantaneous modal parameters identified from experimental data.

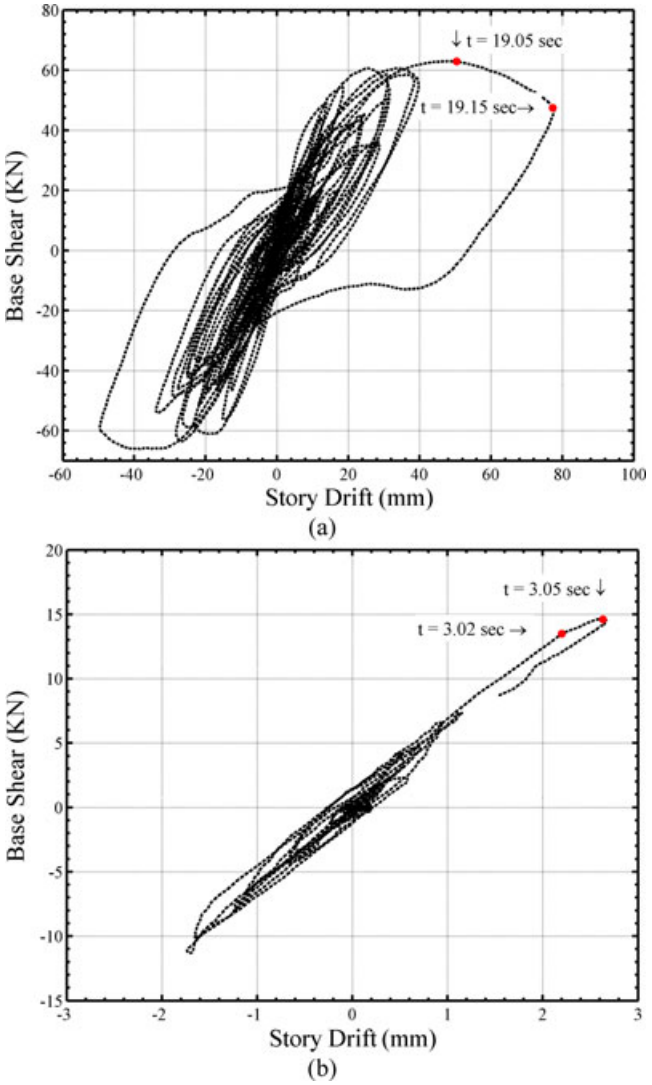

Fig. 18. Hysteretic loops between story drift and base shear: (a) $0 < t < 30$ seconds; (b) $0 < t < 3.18$ seconds.

frequencies are close to the peak frequencies observed in the Fourier spectra (Figure 16). The range of identified ξ in the "before-damage" test is 3.3–10% and that for ξ from the "after-damage" test is 4.4–16%. As expected, the damaged specimen consumes more damping energy than the specimen before damage when subjected to the same level of input acceleration.

The instantaneous natural frequencies from the "during-earthquake" test are close to those identified from the "before-damage" test when $t < 2$ seconds as no damage existed for this duration in the "during-earthquake" test. The value of f_n decreased dramatically around $t = 3$ seconds, which likely indicates specimen damage. As displacement magnitude gradually increases over time to $t = 19.15$ seconds (Figure 15b), the identified f_n value generally decreases to 0.93 Hz and ξ increases to 52% from less than 10%. Subsequently, the gradual decrease in magnitude of displacement responses leads to an increase in f_n and decrease to ξ. These observations obey the well-known physical phenomenon suggesting that structural damage decreases the natural frequency and increases the damping ratio of a structure.

To explain further the identified instantaneous modal parameters in the "during-earthquake" test, Figure 18a depicts experimental hysteretic loops between story drift and base shear. The story drift is the relative displacement between A and B (Figure 14), and base shear was measured from load cells. The plot was constructed by using the measured data from $t = 0$ to 30 seconds. The plot clearly indicates that the specimen was severely damaged during the test. Figure 18b presents an enlarged section of the plot in Figure 18a for $t \leq 3.18$ seconds. Notably, the curve slope at an instant

highly depends on structure stiffness at that time. The slopes of the curve between $t = 3.02$ and 3.05 seconds are significantly smaller than those for $t \leq 3.02$ seconds (Figure 18b). Hence, a remarkable decrease in f_n exists at roughly $t = 3$ seconds (Figure 17). Negative slopes exist along the largest hysteretic loop at $19.05 \leq t \leq 19.15$ (Figure 18a) and result in the smallest f_n (Figure 17). Furthermore, the largest hysteretic loop indicates the largest energy dissipation in the loop and yields the largest damping ratio (Figure 17).

6 CONCLUDING REMARKS

This work presented a novel approach for accurately estimating instantaneous modal parameters of a time-varying structural system via the TVARX model. A moving least-squares technique with polynomial basis functions—frequently utilized in a mesh-free method for analyzing mechanical problems—is adopted to establish the shape functions for the coefficient functions of the TVARX model. The primary advantages of the proposed approach over a conventional basis function expansion approach and a weighted basis function approach are in using low-order polynomial basis functions and in saving computational time, respectively. Finally, the instantaneous natural frequencies and damping ratios are directly estimated from coefficient functions of the TVARX model.

This work theoretically developed the equivalent relations between the equation of motion and the TVARX mode, and further proved that the instantaneous modal parameters of a time-varying system can be estimated from the TVARX model coefficients established from displacement responses—but not from velocity or acceleration responses—via a conventional technique typically utilized to identify modal parameters of the time-invariant ARX model.

To confirm the validity of the proposed identification approach, numerical simulations of a time-varying system with a single degree of freedom were performed. This work numerically demonstrated that the proposed approach is much superior to some existing approaches (i.e., recursive technique with a forgetting factor, traditional basis function expansion approach, and weighted basis function expansion approach) in providing accurate estimation of instantaneous modal parameters for a structure. Numerical studies indicate that increasing the number of nodal points ($\hat{l}$) generally improves the accuracy of identified instantaneous modal parameters. When a large number of nodal points is utilized, the identified instantaneous modal parameters are not significantly affected by the order of polynomial basis functions ($\bar{N}$) and the support of the weight function (d) for $\bar{N} = 0, 1, 2, 3$ and $d = 4$ or 6 seconds. When data containing noise are processed, one must increase the order of the TVARX model to identify the instantaneous modal parameters accurately.

To demonstrate the applicability of the proposed approach to real data, responses to shaking table tests were processed. The specimen was subjected to a series of base excitation inputs. The specimen was first shaken under white noise input with small amplitude, then subjected to a large earthquake input and damaged, and finally shaken under a small amount of white noise input again. The trend in variations of the identified instantaneous modal parameters is consistent with the observed physical phenomena during the tests. Changes to instantaneous modal parameters due to structure damage can be applied to develop useful criteria for assessing damage of real structures.

The work concentrated on a system with a single degree of freedom or a system with single input/output because the resulting mathematical formulation is simple, its correctness is easily verified, and the parameters controlling the accuracy of the identified instantaneous modal parameters can be studied comprehensively. The formulas given here are easily extended to systems with multiple degrees of freedom. Application of the proposed approach to processing measured responses of structures with multiple degrees of freedom and further performing damage assessment of structures are interesting and shall be done in the future.

ACKNOWLEDGMENTS

The authors thank the National Science Council of the Republic of China, Taiwan, for financially supporting this research under Contract No. NSC 94-2625-Z-009-006. The appreciation is also extended to Professor C. H. Loh and the National Center for Research on Earthquake Engineering for providing shaking table test data.

REFERENCES

Adeli, H. & Jiang, X. (2006), Dynamic fuzzy wavelet neural network model for structural system identification, *Journal of Structural Engineering, ASCE*, **132**(1), 102–11.

Adeli, H. & Kim, H. (2004), Wavelet-hybrid feedback least mean square algorithm for robust control of structures, *Journal of Structural Engineering*, **130**(1), 128–37.

Adeli, H. & Saleh, A. (1997), Optimal control of adaptive/smart bridge structures, *Journal of Structural Engineering*, **123**(2), 218–26.

Adeli, H. & Saleh, A. (1998), Integrated structural/control optimization of large adaptive/smart structures, *International Journal of Solids and Structures*, **35**(28–29), 3815–30.

Adeli, H. & Samant, A. (2000), An adaptive conjugate gradient neural network—wavelet model for traffic incident detection, *Computer-Aided Civil and Infrastructure Engineering*, **13**(4), 251–60.

Akaike, H. (1973), Information theory and an extension of the maximum likelihood principle. 2nd *International Symposium on Information Theory*, Akademia Kiado, Budapest, 267–81.

Belge, M. & Miller, E. L. (2000), A sliding window RLS-like adaptive algorithm for filtering alpha-stable noise, *IEEE Signal Process Letter*, **7**(4), 86–89.

Carden, E. P. & Brownjohn, J. M. W. (2008), Fuzzy clustering of stability diagrams for vibration-based structural health monitoring, *Computer-Aided Civil and Infrastructure Engineering*, **23**(5), 360–72.

Choi, B. Y. & Bien, Z. (1989), Sliding-windowed weighted recursive least-squares method for parameter estimation, *Electron Letter*, **25**(20), 1381–82.

Clinton, J. F., Bradford, S. C., Heaton, T. H. & Favela, J. (2006), The observed wander of the natural frequencies in a structure, *Bulletin of the Seismological Society of America*, **96**(1), 237–57.

Fortescue, T. R., Kershenbaum, L. S. & Ydstie, B. E. (1981), Implementation of self-tuning regulators with variable forgetting factors, *Automatica*, **17**(6), 831–35.

Ghosh-Dastidar, S. & Adeli, H. (2003), Wavelet-clustering-neural network model for freeway incident detection, *Computer-Aided Civil and Infrastructure Engineering*, **18**(5), 325–38.

He, X., Moaveni, B., Conte, J. P., Elgamal, A. & Masri, S. F. (2008), Modal identification study of Vincent Thomas bridge using simulated wind-induced ambient vibration data, *Computer-Aided Civil and Infrastructure Engineering*, **23**(5), 373–88.

Huang, C. S. (2001), Structural identification from ambient vibration measurement using the multivariate AR model, *Journal of Sound and Vibration*, **241**(3), 337–59.

Jiang, J. & Cook, R. (1992), Fast parameter tracking RLS algorithm with high noise immunity, *Electron Letter*, **28**(22), 2042–45.

Jiang, X. & Adeli, H. (2008a), Dynamic fuzzy wavelet neuroemulator for nonlinear control of irregular highrise building structures, *International Journal for Numerical Methods in Engineering*, **74**(7), 1045–66.

Jiang, X. & Adeli, H. (2008b), Neuro-genetic algorithm for nonlinear active control of highrise buildings, *International Journal for Numerical Methods in Engineering*, **75**(7), 770–86.

Jiang, X., Mahadevan, S. & Adeli, H. (2007), Bayesian wavelet packet denoising for structural system identification, *Structural Control and Health Monitoring*, **14**, 333–56.

Karim, A. & Adeli, H. (2002), Incident detection algorithm using wavelet energy representation of traffic patterns, *Journal of Transportation Engineering*, **128**(3), 232–42.

Kim, H. & Adeli, H. (2004), Hybrid feedback-least mean square algorithm for structural control, *Journal of Structural Engineering*, **130**(1), 120–27.

Kim, H. & Adeli, H. (2005a), Hybrid control of smart structures using a novel wavelet-based algorithm, *Computer-Aided Civil and Infrastructure Engineering*, **20**(1), 7–22.

Kim, H. & Adeli, H. (2005b), Wavelet hybrid feedback-lms algorithm for robust control of cable-stayed bridges, *Journal of Bridge Engineering*, **10**(2), 116–23.

Kim, H. & Adeli, H. (2005c), Hybrid control of irregular steel highrise building structures under seismic excitations, *International Journal for Numerical Methods in Engineering*, **63**(12), 1757–74.

Kim, H. & Adeli, H. (2005d), Wind-induced motion control of 76-story benchmark building using the hybrid damper-tuned liquid column damper system, *Journal of Structural Engineering*, **131**(12), 1794–1802.

Lancaster, P. & Šalkauskas, K. (1990), *Curve and Surface Fitting—An Introduction*, Academic Press, NY.

Leung, S. H. & So, C. F. (2005), Gradient-based variable forgetting factor RLS algorithm in time-varying environments, *IEEE Transactions on Signal Processing*, **53**(8), 3141–50.

Li, S. & Wu, Z. (2008), A non-baseline method for damage locating and quantifying in beam-like structure based on dynamic distributed strain measurements, *Computer-Aided Civil and Infrastructure Engineering*, **23**(5), 404–13.

Liu, G. R. (2003), *Mesh Free Methods: Moving Beyond the Finite Element Method*, CRC Press, NY.

Ljung, L. (1987), *System Identification*, *Theory for the User*, Prentice-Hall, Englewood Cliffs, NJ.

Loh, C. H., Lin, C. Y. & Huang, C. C. (2000), Time domain identification of frames under earthquake loadings, *Journal of Engineering Mechanics*, *ASCE*, **126**(7), 693–703.

Marmarelis, V. Z. (1987), *Advanced Methods of Physiological System Modeling*, University of Southern California, Los Angeles.

Moaveni, B., He, X., Conte, J. P. & de Callafon, R. A. (2008), Damage identification of a composite beam based on changes of modal parameters, *Computer-Aided Civil and Infrastructure Engineering*, **23**(5), 339–59.

Ni, Y. Q., Zhou, H. F., Chan, K. C., & Ko, J. M. (2008), Modal flexibility analysis of cable-stayed Ting Kau bridge for damage identification, *Computer-Aided Civil and Infrastructure Engineering*, **23**(3), 223–36.

Niedźwiecki, M. (1988), Functional series modelling approach to identification of nonstationary stochastic systems, *IEEE Transactions Automatic Control*, **33**, 955–61.

Niedźwiecki, M. (2000), *Identification of Time-Varying Processes*, John Wiley & Sons, NY.

Park, D. J. & Jun, B. E. (1992), Self-perturbing recursive least squares algorithm with fast tracking capability, *Electron Letter*, **28**(6), 558–59.

Salawu, O. S. (1997), Detection of structural damage through changes in frequency: a review, *Engineering Structures*, **19**, 718–23.

Saleh, A. & Adeli, H. (1994), Parallel algorithms for integrated structural and control optimization, *Journal of Aerospace Engineering*, **7**(3), 297–314.

Saleh, A. & Adeli, H. (1997), Robust parallel algorithms for solution of the Riccati equation, *Journal of Aerospace Engineering*, **10**(3), 126–33.

Saleh, A. & Adeli, H. (1998), Optimal control of adaptive building structures under blast loading, *Mechatronics*, **8**(8), 821–44.

Toplis, B. & Pasupathy, S. (1988), Tracking improvements in fast RLS algorithm using a variable forgetting factor, *IEEE Trans Acoust Speech Signal Process*, *ASSP*, **36**(2), 206–27.

Tsatsanis, M. K. & Giannakis, G. B. (1993), Time-varying system identification and model validation using wavelets, *IEEE Transactions Signal Processing*, **41**, 3512–23.

Wang, Z. H. & Fang, T. (1986), A time-domain method for identifying modal parameters, *Journal of Applied Mechanics*, **53**, 159–65.

Watson, G. A. (1980), *Approximation Theory and Numerical Methods*, John Wiley & Sons, NY.
Wei, H.-L. & Billings, S. A. (2002), Identification of time-varying systems using multiresolution wavelet models, *International Journal of Systems Science*, **33**(15), 1217–28.
Wu, C. L., Yang, Y. S. & Loh, C. H. (2006), Dynamic gravity load collapse of non-ductile RC frames I: experimental approach, *Proceedings of the 8th U.S. National Conference on Earthquake Engineering*, paper no. 750.
Zou, R., Wang, H. & Chon, K. H. (2003), A robust time-varying identification algorithm using basis functions, *Annals of Biomedical Engineering*, **31**, 840–53.

APPENDIX

Nomenclature

$a(t)$ = acceleration
$a_g(t)$ = base excitation input
$\boldsymbol{a}_i$ = coefficient vector corresponding to $\boldsymbol{p}_i$
$a_n(t)$ = residual error in TVARX
$c(t)$ = damping coefficient, function of time
d = support of weight function
$f(t-i)$ = input at time $t - i\,\Delta t$
f_n = instantaneous natural frequency (Hz)
(I, J) = order of TVARX
$k(t)$ = stiffness, function of time
$\bar{l}_i$ = the number of nodal points for $\phi_i(t)$
$\hat{l}_j$ = the number of nodal points for $\theta_j(t)$
$m(t)$ = mass, function of time
N_i = the highest order of polynomial in $\boldsymbol{p}_i$
$\bar{N}_j$ = the highest order of polynomial in $\bar{\boldsymbol{p}}_j$
$\bar{N}$ = N_i and $\bar{N}_j$ for all i and j
$\boldsymbol{p}_i$ = a vector of polynomial basis functions for $\phi_i(t)$
$\bar{\boldsymbol{p}}_j$ = a vector of polynomial basis functions for $\theta_j(t)$
$v(t)$ = velocity
$W(t, t_l)$ = a weight function
$x(t)$ = displacement
$y\,(t-i)$ = measured response at time $t - i\Delta t$
$\omega_n(t)$ = instantaneous natural frequency (rad/second)
ω_{1a} = instantaneous natural frequency identified by using acceleration responses
ω_{1v} = instantaneous natural frequency identified by using velocity responses
$\xi(t)$ = instantaneous damping ratio
ξ_{1a} = instantaneous damping ratio identified by using acceleration responses
ξ_{1v} = instantaneous damping ratio identified by using velocity responses
$\phi_i(t), \theta_j(t)$ = coefficient functions in TVARX
$\tilde{\phi}_{ik}$ = true values of $\phi_i(t_k)$
$\tilde{\theta}_{jk}$ = true values of $\theta_j(t_k)$
$\tilde{\boldsymbol{\varphi}}_i(t)$ = a vector of shape functions for $\phi_i(t)$
$\tilde{\boldsymbol{\theta}}_j(t)$ = a vector of shape functions for $\theta_j(t)$
μ = means of relative error in identifying instantaneous modal parameters
$\bar{\mu}$ = an error index defined by Equation (46)
σ = variances of relative error in identifying instantaneous modal parameters